PHYSICAL REVIEW D **96,** 104030 (2017)

General relativistic observable for gravitational astrometry in the context of the Gaia mission and beyond

Mariateresa Crosta,* Andrea Geralico, Mario G. Lattanzi, and Alberto Vecchiato

Astrophysical Observatory of Turin (OATo)—INAF, via Osservatorio 20, I-10025 Pino Torinese (TO), Italy

(Received 26 July 2017; published 17 November 2017)

With the launch of the Gaia mission, general relativity (GR) is now at the very core of astrometry. Given the high level of accuracy of the measurements, the development of a suitable relativistic model for carrying out the correct data processing and analysis has become a critical necessity; its primary goal is to have a consistent set of stellar astrometric parameters by which to map a relativistic kinematic of a large portion of the Milky Way and, therefore, taking the first step of the cosmic distance ladder to higher accuracy. To trace light trajectories back to the emitting stars requires an appropriate treatment of local gravity and a relativistic definition of the observable, according to the measurement protocol of GR, so that astrometry cannot be set apart from fundamental physics. Consequently, the final Gaia outputs, following completion of its operational life, will have important new implications and an overwhelming potential for astrophysical phenomena requiring the highest precision. In this regard, the present work establishes the background GR procedure to treat such relativistic measurements from within the weak gravitational field of the Solar System. In particular, we make the method explicit in the framework of the RAMOD relativistic models, consistent with the IAU (standard) resolutions and, therefore, suitable for validating the GREM approach baselined for Gaia.

DOI: 10.1103/PhysRevD.96.104030

I. INTRODUCTION

Gaia, of the European Space Agency (ESA), is the first astrometric mission of the twenty-first century and was successfully launched on December 19, 2013. The challenging astrometric goal of the mission is the census of about two billion individual stars comprising the Milky Way (MW) to be materialized in the form of a catalog that will list, for each entry, the five fundamental astrometric parameters: two angular coordinates (providing a direction), the parallax, and the two components of annual proper motion [1,2]. Gaia is a spinning two-telescope astrometric system imaging two fields-of-view (FOVs), separated by a large angle (indispensable for absolute parallaxes), on to the same focal plane. In addition, a special scanning law (that combines a six-hour spin period of the two-telescope optical assembly with a 5.8 revolutions/year precession of the same axis at a fixed 45° angle to the Sun) ensures a repeated 4π coverage of the celestial sphere over the satellite's operational lifetime. In five years, each detected object is expected to be observed, on average, 70 times, leading to a total of more than 150 billion measurements. At the end of the mission, astrometric accuracies are expected to be better than 5–10 microarcseconds (μas) for the brighter stars and 130– 600 μas for faint targets, with red objects better measured than bluer ones.

Since the location of an object in astrophysical astrometry is considered reliable if its relative error is better than 10%, performing parallaxes to 10 μas or better implies reaching the kpc scale, i.e., the Galactic scale. Therefore, thanks to the depth of the MW probed with precision parallaxes, space motions (including radial velocities whenever possible), and astrophysical characterization (through spectrophotometry) for such an unprecedented sample of individual stars, Gaia will have a huge impact across many fields. These include many branches of stellar astrophysics (details of the structure and stellar evolutionary phases), exoplanets (about 15000 within 200–500 pc), solar system objects, the cosmic distance ladder (through a superb astrometric characterization, i.e., model independent, of the primary calibrators such as Cepheids), and fundamental physics. Gaia will not only greatly enhance our knowledge of the Galactic structure, but it will also provide precise information allowing astronomers to frame a much more detailed kinematical picture of our Galaxy than ever before. For instance, new "accurate" distances and motions of the stars within our Galaxy will provide access to the cosmological signatures left in the disk and halo, offering independent, direct and detailed comparisons of the predictions of the most advanced cosmological simulations [3].

On September 14, 2016, the first catalogue, TGAS, was released to the scientific community worldwide ([4,5]). The five-parameter astrometric solution for two million stars in common between the Tycho-2 Catalogue and Gaia were collected, complete down to magnitude 9—solar neighborhood, open clusters and associations, moving groups, etc.—with submilliarcsec accuracy (10% at 300 pc). Although TGAS has not yet achieved the final expected accuracy, it

*crosta@oato.inaf.it

represents a first return from the Gaia data that already shows the mission is fulfilling its promise.

Nevertheless, a six-dimensional accurate reconstruction of the individual stars across a large portion of the Milky Way necessarily needs extremely accurate astrometric observations modeled within a fully, comparably accurate, relativistic framework. Indeed, at the microarcsecond level of accuracy, a fully relativistic inverse ray-tracing methodology is required in accordance with the local geometrical environment affecting light propagation itself and at the observer's gravitational location, i.e., a correct application of the precepts of the theory of measurement in general relativity (GR) [6]. Consequently, rigorous models of the Gaia observables consistent with the precepts of GR and the relativistic consistency of the whole data processing chain are both indispensable prerequisites for the physically correct achievement of Gaia's goals.

Given the absolute character of the results, the DPAC (Data Processing and Analysis Consortium, i.e., the international consortium which is in charge of the reduction of the Gaia data [7]) decided two procedures for the sphere reconstruction task: one by the Astrometric Global Iterative Solution (AGIS,[8]) and the other by the Global Sphere Reconstruction (GSR, [9,10]), an independent procedure for validation purposes. This approach brings some similarities with the strategy adopted for the HIPPARCOS mission. In that case, two different consortia (FAST and NDAC) prepared two complete and independent data reduction pipelines. In the case of Gaia, it was decided to replicate the baseline process AGIS by implementing GSR, which uses different astrometric models and different algorithms, as part of the so-called Astrometric Verification Unit (AVU).

In the Gaia context, the practical realization of the celestial sphere is an extremely challenging problem because of the high quality of the observations and the large number of unknowns involved. The former issue implies that the aforementioned accurate relativistic astrometric model has to be adequately used, while the huge number of unknowns and observations puts this task at the forefront of high-performance computing problems [11]. Finally, this reconstruction allows, as a byproduct, a high-accuracy estimation of the PPN γ parameter at the 10^{-6} level, and thus represents a high-accuracy test of gravity theories by itself [12]. Moreover, the scientific validation of the sphere reconstruction will involve both a mutual verification of the AGIS and GSR results and several comparisons with external data.

This paper is the development of the GSR astrometric model suitable for the AVU purpose within the framework of the General Relativistic Astrometric MODels (RAMOD), a family with increasing intrinsic accuracy adapted to many different observer's settings, interfacing numerical and analytical relativity and based on the measurement protocol of classical general relativity.

RAMOD was initially developed to finalize consistently with GR the sphere reconstructions within AVU, but it actually describes, in a relativistically rigorous way, the null geodesics in the weak field regime at different levels of accuracy for the first linear perturbations of the metric, and different models of the family can be adopted according to the needs of a specific problem or measurements in the Solar System. For example, in principle, RAMOD3a (see Crosta *et al.*, 2015, and references therein [13]), a static model at the ϵ^2 level (where $\epsilon \equiv v/c$), should be sufficient for the sphere reconstruction at the Gaia accuracy of GSR, and RAMOD3b/4a (ϵ^3) will be used if the retarded distances need to be included appropriately, because it is able to consider them in a more rigorous way. Dynamical models like RAMOD4 (up to ϵ^4) could be suitable, for example, for taking into account gravitomagnetic relativistic effects. The modular structure of GSR, moreover, allows one to implement different astrometric models, thus transforming this pipeline in a sort of machinery for the numerical testing of different relativistic models. Here we adapt the RAMOD3/4 solutions in GSR in order to produce a validation Gaia catalogue and compare its outputs with those of the GREM baselined model of AGIS. The resulting catalog will be expressed in the BCRS coordinates of the IAU resolutions [14].

Despite the fact that this issue might seem rather technical, we wish to stress that from the theoretical, computational, and experimental points of view, relativistic astrometry is opening largely uncharted territory. Stemming from the Gaia needs, there now exist different ways to model light propagation observables in the context of GR [15–17]. Their multiple and simultaneous availability is needed in order to rule out possible spurious contributions (especially systematic errors due to, e.g., insufficient instrumental modeling) and to consolidate the future experimental results, particularly if one is required to take into account and to implement gravitational source velocities and retarded time effects; these manifest themselves in the weak gravitational fields of the Solar System, which turns out to be "strong" already at the level of the accuracy expected for Gaia, namely $(v/c)^3$. Light tracing can be affected by such ever-present and ever-changing gravitational perturbations interfering with the accurate physical interpretation of the measurements, especially in the case of a continuous whole sky coverage.

Section II is devoted to summarize the GR light-tracing from within the IAU metric of the Solar System in the RAMOD context, and Sec. III puts in the same framework the relativistic observation for a Gaia-like observer. Section IV details the relativistic observation equations needed to solve the astrometric problem for AVU/GSR, while Sec. V shows the numerical consistency of the new relativistic algorithms with the intrinsic accuracy of the RAMOD/IAU adopted relativistic model and their validation with respect to GREM. Finally, in Sec. VI, we remark

on the impact of such a relativistic procedure beyond the immediate scope of the AVU/GSR astrometric solution.

II. INVERSE RAY-TRACING FROM WITHIN WEAK GRAVITATIONAL FIELDS

A. Spacetime metric in the global and local coordinate system

Given a geometrical background, analytical solutions of the null geodesic provide the light directions that can be implemented in the relativistic modeling of astronomical observables. As far as the Solar System is concerned, the background spacetime consists of N gravitationally interacting bodies, each associated with its own world lines $\mathcal{L}_{(a)}$ ($a = 1 \ldots N$). Here, we choose to neglect the multipolar fields defined along it.

It is customary to identify a "global coordinate system" $x^\alpha = (ct, x^i)$ (with the origin at the center-of-mass) and N local coordinate systems $X^\alpha_{(a)} = (cT_{(a)}, X^a_{(a)})$ for each single body. A mapping between the global and local set of coordinates is given by [18] (Damour-Soffel-Xu formalism, hereafter DSX)

$$\begin{aligned} x^\mu_{(a)} &= x^\mu(cT_{(a)}, X^i_{(a)}) \\ &= z^\mu_{(a)}(cT_{(a)}) + e^\mu_i(cT_{(a)})X^i_{(a)} + \xi^\mu(cT_{(a)}, X^i_{(a)}), \\ \xi^\mu &= O[(X^i_{(a)})^2], \end{aligned} \tag{1}$$

where $z^\alpha_{(a)} = z^\alpha_{(a)}(\tau_{(a)})$ is the parametric equations of $\mathcal{L}_{(a)}$ (with $\tau_{(a)}$ proper time), $e^\mu_i(cT_{(a)})$ denotes a triad of spacelike vectors ($i = 1, 2, 3$) undergoing some geometric transport (e.g., Fermi transport) along the line $\mathcal{L}_{(a)}$.

The gravitational fields interact weakly if the spacetime region of interest can be assumed to be not too close to any given body, so that the metric results as the sum of the Minkowskian metric $\eta_{\alpha\beta} = \mathrm{diag}[-1, 1, 1, 1]$ and small perturbations given as

$$g_{\alpha\beta} = \eta_{\alpha\beta} + h_{\alpha\beta} \tag{2}$$

and can be expressed either in the global coordinates x^μ or in any of the N local coordinates $X^\mu_{(a)}$. The choice of coordinates is actually a gauge choice. In fact, the form of the metric can be very different within different coordinate systems. A minimal request is that it admits a PN expansion in the usual sense,

$$h_{00} = O(c^{-2}), \quad h_{0i} = O(c^{-3}), \quad h_{00} = O(c^{-2}), \tag{3}$$

in each of these coordinate systems. Following DSX, in all coordinate systems we require the spatial coordinates to be "conformally Cartesian" or "isotropic,"

$$g_{00}g_{ij} = -\delta_{ij} + O(1/c^4). \tag{4}$$

This condition imposes severe restrictions on the various elements z^μ, e^μ_a, ξ^μ entering the map between the global coordinates and any of the local ones. However, while standard gauges (harmonic, standard PN gauges) impose differential conditions on the metric, DSX conditions are instead purely algebraic and, hence, more flexible.

Furthermore, at the level of Gaia accuracy, each source can be assumed to move with a constant velocity relative to the global reference system, i.e., $\tilde{v}^i_{(a)} = \mathrm{const}$, where $\tilde{v}^i_{(a)}$ are the coordinate components of the spatial velocity of the ath source, with 4-velocity $\tilde{\mathbf{u}}$ (see Sec. II B). In this case, the transformation between local coordinates $X^\mu = (cT, X^i)$ (where the body is at rest) to global coordinates $x^\mu = (ct, x^i)$ (where the body moves with constant velocity) is given by a Lorentz transformation, i.e.,

$$x^\mu(X^\alpha) = x^\mu_0 + \Lambda^\mu{}_\nu X^\nu, \tag{5}$$

such that for the body

$$\tilde{x}^i(t) = \tilde{x}^i_0 + \tilde{v}^i(t - t_0) + O(\tilde{v}^2). \tag{6}$$

According to DSX the transformation law of the canonical form of the metric perturbation in the local coordinates $X^\mu = (cT, X^i)$ in the exterior region of the matter field can be written as

$$h^{\mu\nu}_{\mathrm{can}}(ct, x^i) = \Lambda^\mu{}_\alpha \Lambda^\nu{}_\beta h^{\alpha\beta}_{\mathrm{can}}(cT, X^i). \tag{7}$$

In the simplest case of an extended body with monopole structure one obtains

$$\begin{aligned} &h^{\mu\nu}_{\mathrm{mono}}(ct, x^i) \\ &\quad = 2G\mathcal{M}\epsilon^2[\gamma(r(t_{\mathrm{ret}}) - \epsilon\tilde{\mathbf{v}}\cdot\mathbf{r}(t_{\mathrm{ret}}))]^{-1}(\eta^{\mu\nu} + 2\epsilon^2\tilde{u}^\mu\tilde{u}^\nu). \end{aligned} \tag{8}$$

Replacing then the retarded time t_{ret} with t in the retarded distance (see Appendix A)

$$\begin{aligned} r^i(t_{\mathrm{ret}}) &= r^i(t) + \epsilon r(t)\tilde{v}^i + \epsilon^2(\mathbf{r}(t)\cdot\tilde{\mathbf{v}})\tilde{v}^i + O(\epsilon^3), \\ r(t_{\mathrm{ret}}) &= r(t)\left[1 + \epsilon\tilde{\mathbf{v}}\cdot\mathbf{n}(t) + \frac{1}{2}\epsilon^2\tilde{v}^2 + \frac{1}{2}\epsilon^2(\tilde{\mathbf{v}}\cdot\mathbf{n}(t))^2\right], \\ &\quad + O(\epsilon^3), \end{aligned} \tag{9}$$

so that

$$\tilde{\mathbf{v}}\cdot\mathbf{r}(t_{\mathrm{ret}}) = r(t)[\tilde{\mathbf{v}}\cdot\mathbf{n}(t) + \epsilon\tilde{v}^2 + \epsilon^2\tilde{v}^2(\tilde{\mathbf{v}}\cdot\mathbf{n}(t))] + O(\epsilon^3). \tag{10}$$

The latter approximations allow to make explicit the retarted time dependency on the coordinate time in the metric coefficient at the accuracy level targeted for a Gaia-like observer and according to the present IAU resolutions for the BCRS metric [14], namely

$$\begin{aligned} g_{00}(ct,x^i) &= -1+2\epsilon^2 h_{(a)}(t,x^i)+O(4),\\ g_{0i}(ct,x^i) &= -4\epsilon^3 h_{(a)}(t,x^i)\tilde{v}^i_{(a)}+O(4),\\ g_{ij}(ct,x^i) &= \delta_{ij}[1+2\epsilon^2 h_{(a)}(t,x^i)]+O(4), \end{aligned} \tag{11}$$

where

$$h_{(a)}(t,x^i)=\frac{G\mathcal{M}_{(a)}}{r_{(a)}(t,x^i)}, \tag{12}$$

$$r_{(a)}(t,x^i)=[(x-x_a(t))^2+(y-y_a(t))^2+(z-z_a(t))^2]^{1/2}. \tag{13}$$

This is the form of the metric extensively used in the literature (see, e.g., Ref [17,19–23]) to which we refer in order to compare RAMOD/GSR results with those of GREM/AGIS. In the following we remove the subscript (a) for simplicity, and, where not useful, we retain terms up to the order of $O(\epsilon^3)$ in the expansion of perturbation quantities.

B. Fiducial observers and BCRS frame

RAMOD framework is based on the measurement protocol in GR [6]. This implies the determination of a set of fiducial observers in order to define measurements all along the light trajectories—from the observer up to the star—with respect to a common rest space. We remind the reader that GR is based on covariant equations for different observers, instead, the goal of an astrometric catalogue is to fix coordinate quantities related to the stars. Then the crucial point is to correctly match these two requirements.

Following the IAU resolutions, RAMOD assumes as fiducial observers those at rest with respect to the center-of-mass (CM) of the BCRS, viz. the static observer with associated 4-velocity

$$u^\alpha=\frac{1}{\sqrt{-g_{00}}}\partial_0^\alpha\approx(1+\epsilon^2 h)\partial_0^\alpha, \tag{14}$$

denoted as "local barycentric observer."

Note that the congruence of curves $\mathbf{u}$ is in general not vorticity-free at the microarcsecond level of accuracy, because of the term $\omega_{ij}(u)=\partial_{[i}h_{j]0}$; i.e., locally and only locally $\mathbf{u}$ is at rest with respect to the CM chosen as origin of the coordinate system.

However, if one compares the scale of the Solar System and the photon crossing time through it—approximately 10 hours in total- the gravitational field of the Solar System cannot significantly change in a dynamical sense during such a time. Then when a photon approaches the weak gravitational field of the Solar System, practically for a Gaia-like observer it will be subjected to the gravitational field generated by the masses of the bodies in the system while being rather insensitive to their own motion. This approximation fits well for the case of constant velocity discussed above and allows to neglect the locality of the vorticity of $\mathbf{u}$ consistently with the purpose of this paper, i.e., a straight comparison between RAMOD and GREM approaches in the IAU framework.

C. Photon trajectories in the RAMOD/IAU framework

The fundamental unknown of the RAMOD approach is the space-like four-vector $\bar{\ell}^\alpha$, which is the projection of the tangent to the null geodesic onto the rest-space of the local barycentric observer, namely the one locally at rest with respect to the barycenter of the Solar System. Physically, such a four-vector identifies the *line-of- sight* of the incoming photon relative to that observer.

Let the null geodesic of the photon be described by the tangent vector field k^α, i.e.,

$$k^\alpha\nabla_\alpha k^\beta=0, \qquad k^\alpha k_\alpha=0, \tag{15}$$

∇_α being the covariant derivative associated with the spacetime metric. The RAMOD decomposition of the photon 4-momentum with respect to the fiducial observer can be denoted as

$$k^\alpha=-(u\cdot k)u^\alpha+\ell^\alpha\equiv\mathcal{E}(k,u)u^\alpha+\ell^\alpha. \tag{16}$$

The trajectory can be parametrized by a parameter σ such that

$$\bar{k}^\alpha=\frac{k^\alpha}{\mathcal{E}(k,u)}=\frac{\mathrm{d}x^\alpha}{\mathrm{d}\sigma}, \tag{17}$$

implying that Eq. (15) becomes

$$\bar{k}^\alpha\nabla_\alpha\bar{k}^\beta=-\frac{\mathrm{d}\ln\mathcal{E}(k,u)}{\mathrm{d}\sigma}\bar{k}^\beta. \tag{18}$$

Correspondingly we can define the previous equations for $\bar{\ell}^\alpha$, so the null geodesic reads for each value of α [13,24] as:

$$\frac{d\bar{\ell}^\alpha}{d\sigma}+\frac{du^\alpha}{d\sigma}-(\bar{\ell}^\alpha+u^\alpha)(\bar{\ell}^\beta\dot{u}_\beta+\bar{\ell}^\beta\bar{\ell}^\tau\nabla_\tau u_\beta)+\Gamma^\alpha_{\beta\gamma}(\bar{\ell}^\beta+u^\beta)(\bar{\ell}^\gamma+u^\gamma)=0. \tag{19}$$

Neglecting all the $O(h^2)$ terms and taking into account that $\bar{\ell}^0=h_{0i}\bar{\ell}^i+O(h^2)$, the solutions of the photon equation of motion are given by

$$\frac{\mathrm{d}x^0}{\mathrm{d}\sigma}=\bar{\ell}^0(\sigma)+1+\epsilon^2h(\sigma),\qquad \frac{\mathrm{d}x^a}{\mathrm{d}\sigma}=\bar{\ell}^a(\sigma). \tag{20}$$

To the order $O(\epsilon^3)$, we then have

$$\bar{\ell}^a=\bar{\ell}^a_\varnothing+\epsilon^2\bar{\ell}^a_{(2)}+\epsilon^3\bar{\ell}^a_{(3)},\qquad x^\alpha=x^\alpha_\varnothing+\epsilon^2x^\alpha_{(2)}+\epsilon^3x^\alpha_{(3)}, \tag{21}$$

where $\bar{\ell}^a_\varnothing$ denotes the unperturbed local photon direction and the parameter σ of the light ray trajectory is fixed so that it is $\sigma=0$ at the event of observation with coordinates $x^\alpha_{\mathrm{obs}}=(x^0_{\mathrm{obs}},x^i_{\mathrm{obs}})$. Therefore, the unperturbed orbit can be written as

$$x^0_\varnothing=x^0_{\mathrm{obs}}+\sigma,\qquad x^a_\varnothing=x^a_{\mathrm{obs}}+\bar{\ell}^a_\varnothing\sigma, \tag{22}$$

with $x^\alpha_{(2)}(0)=0$ and $x^\alpha_{(3)}(0)=0$.

The "actual" locally spatial photon direction evaluated at the observation point $\bar{\ell}^a_{\mathrm{obs}}=\bar{\ell}^a_\varnothing+\epsilon^2\bar{\ell}^a_{(2)}(0)+\epsilon^3\bar{\ell}^a_{(3)}(0)$ has to be considered as known, being related to the direct measurement and to the selected attitude of the observer's frame.

To the order $O(\epsilon^3)$ Eq. (19) for $\bar{\ell}^a$ becomes

$$\frac{\mathrm{d}\bar{\ell}^a}{\mathrm{d}\sigma}=\epsilon^2[2\partial_ah-3\bar{\ell}^a_\varnothing\bar{\ell}^b_\varnothing\partial_bh]+\epsilon^3[-4(\bar{\ell}_\varnothing\cdot\tilde{\mathbf{v}})\partial_ah+4\tilde{v}^a\bar{\ell}^b_\varnothing\partial_bh-\bar{\ell}^a_\varnothing\partial_th] \tag{23}$$

$$=\epsilon^2\left[2\partial_ah-3\bar{\ell}^a_\varnothing\frac{\mathrm{d}h}{\mathrm{d}\sigma}\right]+\epsilon^3\left[-4(\bar{\ell}_\varnothing\cdot\tilde{\mathbf{v}})\partial_ah+4\tilde{v}^a\frac{\mathrm{d}h}{\mathrm{d}\sigma}+2\bar{\ell}^a_\varnothing\partial_th\right]+O(\epsilon^4), \tag{24}$$

where we have used the relation

$$\frac{\mathrm{d}h}{\mathrm{d}\sigma}=\bar{\ell}^i_\varnothing\partial_ih+\epsilon\partial_th+O(\epsilon^2), \tag{25}$$

whereas

$$\bar{\ell}^0(\sigma)=-4\epsilon^3(\bar{\ell}_\varnothing\cdot\tilde{\mathbf{v}})h(\sigma). \tag{26}$$

Note that the eq. (23) has the same form of eq. (22) in [13] neglecting terms of the order of ϵ^4.

Once one introduces the following integral quantities

$$H(\sigma)=\int_0^\sigma h(\sigma)\mathrm{d}\sigma,\qquad H^a(\sigma)=\int_0^\sigma[\partial_ah](\sigma)\mathrm{d}\sigma,$$
$$\mathcal{H}^a(\sigma)=\int_0^\sigma H^a(\sigma)\mathrm{d}\sigma,\qquad H^t(\sigma)=\int_0^\sigma[\partial_th](\sigma)\mathrm{d}\sigma,$$
$$\mathcal{H}^t(\sigma)=\int_0^\sigma H^t(\sigma)\mathrm{d}\sigma, \tag{27}$$

the solution is then formally given by

$$\bar{\ell}^a(\sigma)=\bar{\ell}^a_{\mathrm{obs}}+\epsilon^2\{2[1-2\epsilon(\tilde{\mathbf{v}}\cdot\bar{\ell}_\varnothing)]H^a(\sigma)-(3\bar{\ell}^a_\varnothing-4\epsilon\tilde{v}^a)(h(\sigma)-h_{\mathrm{obs}})\}+2\epsilon^3\bar{\ell}^a_\varnothing H^t(\sigma), \tag{28}$$

so that the trajectory results in

$$x^a(\sigma)=x^a_{\mathrm{obs}}+\bar{\ell}^a_{\mathrm{obs}}\sigma+\epsilon^2\{2[1-2\epsilon(\tilde{\mathbf{v}}\cdot\bar{\ell}_\varnothing)]\mathcal{H}^a(\sigma)-(3\bar{\ell}^a_\varnothing-4\epsilon\tilde{v}^a)(H(\sigma)-h_{\mathrm{obs}}\sigma)\}+2\epsilon^3\bar{\ell}^a_\varnothing\mathcal{H}^t(\sigma), \tag{29}$$

whereas

$$x^0(\sigma)=x^0_{\mathrm{obs}}+\sigma+\epsilon^2[1-4\epsilon(\tilde{\mathbf{v}}\cdot\bar{\ell}_\varnothing)]H(\sigma). \tag{30}$$

Finally, the normalization factor $\mathcal{E}(K,u)$ satisfies the equation

$$\frac{\mathrm{d}\mathcal{E}}{\mathrm{d}\sigma}=\epsilon^2\bar{\ell}^i_\varnothing\partial_ih-\epsilon^3\partial_th=\epsilon^2\frac{\mathrm{d}h}{\mathrm{d}\sigma}-2\epsilon^3\partial_th+O(\epsilon^4), \tag{31}$$

with solution

$$\mathcal{E}(K,u)=1+\epsilon^2(h(\sigma)-h_{\mathrm{obs}})-2\epsilon^3H^t(\sigma), \tag{32}$$

where the unperturbed value has been set equal to unity without any loss of generality.

1. Light trajectories for N-body system with constant velocities

Denoting $x^i-x^i_{(a)}\equiv r^i_{(a)}$, $x^i_{\mathrm{obs}}-x^i_{(a)}\equiv r^i_{\mathrm{obs}}$, and $n^i=r^i/r$, dropping the summation symbol, and the subscript (a), the solutions for n-mass monopoles with constant velocities to be implemented in the astrometric problem for the RAMOD/IAU framework are (more details in Appendix B):

$$
\begin{aligned}
\bar{\ell}^0 &= -4GM\epsilon^3\frac{\bar{\ell}_\oslash\cdot\tilde{\mathbf{v}}}{r},\\
\bar{\ell}^a-\bar{\ell}^a_{\rm obs} &= -GM\epsilon^2\left\{\left(\frac{1}{r}-\frac{1}{r_{\rm obs}}\right)\left[\bar{\ell}^a_\oslash-2\epsilon\left(2d^a_v-\frac{d^a}{d^2}(\tilde{\mathbf{v}}\cdot\mathbf{r}_{\rm obs})\right)\right]+2\frac{d^a}{d^2}[1-2\epsilon(\tilde{\mathbf{v}}\cdot\bar{\ell}_\oslash)](\mathbf{n}\cdot\bar{\ell}_\oslash-\mathbf{n}_{\rm obs}\cdot\bar{\ell}_\oslash)\right\}\\
&\quad+2GM\epsilon^3\frac{r_{\rm obs}}{d^2r}\left[d^a_v-2\frac{d^a}{d^2}(\tilde{\mathbf{v}}\cdot\mathbf{d})\right][r-r_{\rm obs}-(\mathbf{n}_{\rm obs}\cdot\bar{\ell}_\oslash)\sigma],\\
x^0-x^0_{\rm obs} &= \sigma+\epsilon^2GM[1-3\epsilon(\tilde{\mathbf{v}}\cdot\bar{\ell}_\oslash)]\ln\left[\frac{r+(\mathbf{r}\cdot\bar{\ell}_\oslash)}{r_{\rm obs}+(\mathbf{r}_{\rm obs}\cdot\bar{\ell}_\oslash)}\right]+\frac{\epsilon^3GM}{r+(\mathbf{r}\cdot\bar{\ell}_\oslash)}\left\{\frac{r-r_{\rm obs}+\sigma}{r_{\rm obs}+(\mathbf{r}_{\rm obs}\cdot\bar{\ell}_\oslash)}(\tilde{\mathbf{v}}\cdot\mathbf{d})-(\tilde{\mathbf{v}}\cdot\bar{\ell}_\oslash)\sigma\right\},\\
x^a-x^a_{\rm obs} &= \bar{\ell}^a_{\rm obs}\sigma-GM\epsilon^2\left\{\bar{\ell}^a_\oslash\left[[1+\epsilon(\tilde{\mathbf{v}}\cdot\bar{\ell}_\oslash)]\ln\left[\frac{r+(\mathbf{r}\cdot\bar{\ell}_\oslash)}{r_{\rm obs}+(\mathbf{r}_{\rm obs}\cdot\bar{\ell}_\oslash)}\right]-\frac{\sigma}{r_{\rm obs}}\right]+2\frac{d^a}{d^2}[r-r_{\rm obs}-(\mathbf{n}_{\rm obs}\cdot\bar{\ell}_\oslash)\sigma]\right\}\\
&\quad-GM\epsilon^3\left\{\frac{\bar{\ell}^a_{\rm obs}}{r+(\mathbf{r}\cdot\bar{\ell}_\oslash)}\left[\frac{r-r_{\rm obs}+\sigma}{r_{\rm obs}+(\mathbf{r}_{\rm obs}\cdot\bar{\ell}_\oslash)}(\tilde{\mathbf{v}}\cdot\mathbf{d})-(\tilde{\mathbf{v}}\cdot\bar{\ell}_\oslash)\sigma\right]-2d^a_v\left[\ln\left[\frac{r+(\mathbf{r}\cdot\bar{\ell}_\oslash)}{r_{\rm obs}+(\mathbf{r}_{\rm obs}\cdot\bar{\ell}_\oslash)}\right]-2\frac{\sigma}{r_{\rm obs}}\right]\right.\\
&\quad\left.-2\frac{rr_{\rm obs}}{d^2}\left[d^a_v-2\frac{d^a}{d^2}(\tilde{\mathbf{v}}\cdot\mathbf{d})\right](\mathbf{n}\cdot\bar{\ell}_\oslash-\mathbf{n}_{\rm obs}\cdot\bar{\ell}_\oslash)+2\frac{d^a}{d^2r_{\rm obs}}[(\tilde{\mathbf{v}}\cdot\bar{\ell}_\oslash)(\mathbf{r}_{\rm obs}\cdot\bar{\ell}_\oslash)-(\tilde{\mathbf{v}}\cdot\mathbf{d})]\sigma\right\},
\end{aligned}
\tag{33}
$$

where

$$
\begin{aligned}
\sigma &= (\mathbf{r}\cdot\bar{\ell}_\oslash)-(\mathbf{r}_{\rm obs}\cdot\bar{\ell}_\oslash)+O(\epsilon^2)\\
&= (\mathbf{x}-\mathbf{x}_{\rm obs})\cdot\bar{\ell}_\oslash+O(\epsilon^2),
\end{aligned}
\tag{34}
$$

and

$$
\begin{aligned}
d^a &= [\bar{\ell}_\oslash\times(\mathbf{r}_{\rm obs}\times\bar{\ell}_\oslash)]^a\\
&= r^a_{\rm obs}-\bar{\ell}^a_\oslash(\mathbf{r}_{\rm obs}\cdot\bar{\ell}_\oslash)\equiv P(\bar{\ell}_\oslash)^a{}_b r^b_{\rm obs},
\end{aligned}
\tag{35}
$$

$$
d^2 = r^2_{\rm obs}-(\mathbf{r}_{\rm obs}\cdot\bar{\ell}_\oslash)^2,
\tag{36}
$$

represents the impact parameter with respect to the (a)-source (being $P(\bar{\ell}_\oslash)^a{}_b$ the projector orthogonal to $\bar{\ell}_\oslash$), whereas

$$
d^a_v = [\bar{\ell}_\oslash\times(\tilde{\mathbf{v}}\times\bar{\ell}_\oslash)]^a = P(\bar{\ell}_\oslash)^a{}_b\tilde{v}^b,
\tag{37}
$$

is the projected source velocity with respect to the unperturbed light direction.

Setting $\tilde{v}_{(a)}=0$ the static solution is obtained straightly. The spatial component of these equations are equivalent to those compared with the Time Transfer Function approach [25].

Moreover, following Ref. [13,17] equivalently one can parametrize the photon trajectory in terms of the photon impact parameter $\hat{\xi}^i$ w.r.t. to the center-of-mass of the system (which is equivalent to d^i in case of one body), as follows

$$
x^i = \hat{\xi}^i+\int_{\hat{\sigma}}^{\sigma}\bar{\ell}^i d\sigma,
\tag{38}
$$

$\hat{\sigma}$ being the value of the parameter σ at the point of closest approach, so that

$$
r^i = x^i-x^i_{(a)} = \hat{r}^i_p+\bar{\ell}^i_\oslash(\sigma-\hat{\sigma})+O(\epsilon^2),
\tag{39}
$$

where $\hat{r}^i_p=\hat{\xi}^i-x^i_{(a)}$ denotes the relative distance between the point of closest approach and the source position with respect to the origin of BCRS at given reference time. Therefore, the class of solutions in [13], can be reformulated from Eqs. (23) and (27) by replacing $\sigma\to\sigma-\hat{\sigma}\equiv\tau$ and $r^i_{\rm obs}\to\hat{r}^i_p$ and merging all the different levels of accuracy up to ϵ^3 order in the case of metric (8) expressed in IAU coordinates.

III. THE ASTROMETRIC OBSERVABLE FOR A GAIA-LIKE OBSERVER

A. The observable

Given the solution of the null geodesic we need to define a relationship between the unknowns, namely the position and motion of the star, and the observable quantities. Indeed, we need to fix the initial condition in order to guarantee a unique solution of the astrometric problem. These conditions are the components $\bar{\ell}^k_{\rm obs}$ deduced from equations (33) and provided by the satellite observations.

RAMOD relies on the tetrad formalism for the definition of the observable. The observables can be expressed as functions of the direction cosines of the incoming direction k^α with respect to the axes of the spatial triad $\mathbf{E}_{\hat{\mathbf{a}}}$ adapted to the Gaia satellite attitude [26,27], namely a set of three orthonormal spacelike vectors that are comoving with the satellite and define its rest frame. Therefore, the observables are given as follows:

$$\cos\psi_{(\hat{a},k)}|_{\sigma=0} = \left.\frac{P(u_s)_{\alpha\beta}k^\alpha E^\beta_{\hat{a}}}{[P(u_s)_{\alpha\beta}k^\alpha k^\beta]^{1/2}}\right|_{\sigma=0} \tag{40}$$

$\hat{a}$-th being the direction cosine measured by the observer, i.e., the satellite $\mathbf{u}_s$, where all the quantities are obviously computed at the event of the observation and $P(u_s)$ is the operator that projects onto the satellite rest frame.

B. The observer

Given an orthonormal threading frame $\{u, e(u)_{\hat{a}}\}$ along $\mathbf{u}_s$, the (timelike) satellite world line has 4-velocity

$$u^\alpha_s = \gamma(u_s,u)[u^\alpha + \epsilon\nu^\alpha(u_s,u)] \tag{41}$$

where

$$\nu^\alpha(u_s,u) = \nu^\alpha(u_s,u)^{\hat{a}}e(u)_{\hat{a}},$$
$$\gamma(u_s,u) = (1-\epsilon^2\|\nu(u_s,u)\|^2)^{-1/2}, \tag{42}$$

so that $u_s\cdot u_s = -1$. An adapted frame to this world line can be obtained by boosting the orthonormal threading frame $\{u, e(u)_{\hat{a}}\}$ along $\mathbf{u}_s$, i.e.,

$$E^\alpha_{\hat{0}} = u^\alpha_s, \qquad E^\alpha_{\hat{a}} = B^\alpha(u_s,u)e(u)_{\hat{a}}, \tag{43}$$

where

$$E^\alpha_{\hat{a}} = \left[P(u_s) - \frac{\gamma(u_s,u)}{\gamma(u_s,u)+1}\epsilon^2\nu(u,u_s)\otimes\nu(u,u_s)\right]^\alpha{}_\llcorner e(u)_{\hat{a}}, \tag{44}$$

(the symbol $\llcorner$ denotes right contraction) and

$$\epsilon\nu^\alpha(u,u_s) = \frac{1}{\gamma(u_s,u)}u^\alpha - u^\alpha_s. \tag{45}$$

The time component of the satellite 4-velocity (41) is

$$u^0 = 1 + \epsilon^2\left(\frac{1}{2}v^2 + h\right) + O(\epsilon^4), \tag{46}$$

implying that

$$u^\alpha_s = u^0[\partial^\alpha_0 + \epsilon\mathbf{v}^\alpha], \tag{47}$$

where the notation

$$\mathbf{v}^\alpha = v^a\partial^\alpha_a, \qquad v^2 = \delta_{ab}v^av^b \tag{48}$$

has been used and v^a depends on t only. In terms of the coordinate components of the spatial velocity the frame components $\nu^\alpha(u_s,u)^{\hat{a}}$ and the associated Lorentz factor $\gamma(u_s,u)$ are

$$\nu^\alpha(u_s,u)^{\hat{a}} = (1+2h\epsilon^2)\mathbf{v}^\alpha,$$
$$\gamma(u_s,u) = 1 + \frac{v^2}{2}\epsilon^2 + O(\epsilon^4). \tag{49}$$

The spatial triad (44) adapted to $\mathbf{u}_s$ is thus given by

$$\begin{aligned}\tilde{\lambda}^\alpha_{\hat{a}} = E^\alpha_{\hat{a}} &= \left\{\epsilon v^a + \epsilon^3\left[v^a\left(\frac{v^2}{2}+3h\right) - 4h\tilde{v}^a\right]\right\}\partial^\alpha_0 \\ &\quad + (1-\epsilon^2 h)\partial^\alpha_a + v^a\frac{\epsilon^2}{2}\mathbf{v}^\alpha + O(\epsilon^4) \\ &= \lambda^\alpha_{\hat{a}} + \epsilon v^a\left[1+\epsilon^2\left(\frac{v^2}{2}+3h\right)\right]\partial^\alpha_0 + \frac{1}{2}\epsilon^2 v^a v^b\partial^\alpha_b + O(\epsilon^4).\end{aligned} \tag{50}$$

where, according to metric (11),

$$\lambda^\alpha_{\hat{a}} = e(u)_{\hat{a}} = (1-\epsilon^2 h)\partial^\alpha_a - 4\epsilon^3 h\tilde{v}_a\partial^\alpha_0. \tag{51}$$

is the local barycentric observer-adapted orthonormal spatial frame.

C. Gaia's attitude frame and the observables

The astrometric satellite Gaia is expected to orbit the Earth-Sun system at the outer Lagrangian point L2 following a trajectory modulated in three spatial directions. More precisely, the two Gaia Fields of View (FoVs) can sweep the whole celestial sphere approximately every six months thanks to the combination of three independent motions of the satellite: the spin around its z-axis (1 turn every 6 hours), the precession of such an axis around the satellite-Sun direction ($\alpha = 45°$) with a period of 70 days, and the orbital motion around the Sun of its barycenter.

The Gaia attitude frame is specified by the following spatial rotation of the adapted triad (50)

$$F^\alpha_{\hat{a}} = \mathcal{A}(\sigma_i)_{\hat{a}}{}^{\hat{b}}\tilde{\lambda}^\alpha_{\hat{b}}, \tag{52}$$

where

$$\mathcal{A} = \frac{1}{(2-\Sigma)^2}\begin{pmatrix} 4(\sigma_1^2-\sigma_2^2-\sigma_3^2)+\Sigma^2 & 8\sigma_1\sigma_2+4\sigma_3\Sigma & 8\sigma_1\sigma_3-4\sigma_2\Sigma \\ 8\sigma_1\sigma_2-4\sigma_3\Sigma & 4(-\sigma_1^2+\sigma_2^2-\sigma_3^2)+\Sigma^2 & 8\sigma_2\sigma_3+4\sigma_1\Sigma \\ 8\sigma_3\sigma_1+4\sigma_2\Sigma & 8\sigma_3\sigma_2-4\sigma_1\Sigma & 4(-\sigma_1^2-\sigma_2^2+\sigma_3^2)+\Sigma^2 \end{pmatrix}, \tag{53}$$

with $\Sigma = 1 - \sigma_1^2 - \sigma_2^2 - \sigma_3^2$, $\det(\mathcal{A}) = 1$ and $\{\sigma_1, \sigma_2, \sigma_3\}$ are modified Rodrigues parameters.

These latter expressions can then be linked in a standard way to the astrometric unknowns of the observed object [28]. We find

$$\cos\psi_{(\hat{a},k)} = (\mathbf{C}_{\hat{a}}\cdot\bar{\ell})(1+2\epsilon^2 h)[1+\epsilon(\mathbf{v}\cdot\bar{\ell}_\varnothing)] - \epsilon(\mathbf{C}_{\hat{a}}\cdot\bar{\ell}_\varnothing)(1-\epsilon^2 h)(\mathbf{v}\cdot\bar{\ell}_\varnothing) + \epsilon(1+2\epsilon^2 h)[(\mathbf{v}\cdot\bar{\ell})(\mathbf{C}_{\hat{a}}\cdot\bar{\ell}_\varnothing) - \mathbf{C}_{\hat{a}}\cdot\mathbf{v}] + \epsilon^2[1+\epsilon(\mathbf{v}\cdot\bar{\ell}_\varnothing)]\left\{-\frac{1}{2}(\mathbf{v}\cdot\bar{\ell}_\varnothing)(\mathbf{C}_{\hat{a}}\cdot\mathbf{v}) + (\mathbf{C}_{\hat{a}}\cdot\bar{\ell}_\varnothing)\left[(\mathbf{v}\cdot\bar{\ell}_\varnothing)^2 - \frac{v^2}{2}\right]\right\} + O(\epsilon^4), \tag{54}$$

which have to be evaluated at the position of the satellite, i.e., for $\sigma = 0$. The coefficients $C^b_{\hat{a}}$ are functions only of the attitude parameters (σ_1, σ_2, σ_3), and are explicitly given by

$$C^b_{\hat{1}} = \mathcal{A}_{\hat{1}\,\hat{b}}, \qquad C^b_{\hat{2}} = \mathcal{A}_{\hat{2}\,\hat{b}}, \qquad C^b_{\hat{3}} = \mathcal{A}_{\hat{3}\,\hat{b}}, \tag{55}$$

namely

$$\begin{aligned}
C^1_{\hat{1}} &= \frac{4(\sigma_1^2-\sigma_2^2-\sigma_3^2)+\Sigma^2}{(2-\Sigma)^2}, & C^2_{\hat{1}} &= \frac{8\sigma_1\sigma_2+4\sigma_3\Sigma}{(2-\Sigma)^2}, & C^3_{\hat{1}} &= \frac{8\sigma_1\sigma_3-4\sigma_2\Sigma}{(2-\Sigma)^2},\\
C^1_{\hat{2}} &= \frac{8\sigma_1\sigma_2-4\sigma_3\Sigma}{(2-\Sigma)^2}, & C^2_{\hat{2}} &= \frac{4(-\sigma_1^2+\sigma_2^2-\sigma_3^2)+\Sigma^2}{(2-\Sigma)^2}, & C^3_{\hat{2}} &= \frac{8\sigma_2\sigma_3+4\sigma_1\Sigma}{(2-\Sigma)^2},\\
C^1_{\hat{3}} &= \frac{8\sigma_3\sigma_1+4\sigma_2\Sigma}{(2-\Sigma)^2}, & C^2_{\hat{3}} &= \frac{8\sigma_3\sigma_2-4\sigma_1\Sigma}{(2-\Sigma)^2} & C^3_{\hat{3}} &= \frac{4(-\sigma_1^2-\sigma_2^2+\sigma_3^2)+\Sigma^2}{(2-\Sigma)^2}.
\end{aligned} \tag{56}$$

It is worth rewriting Eq. (54) as follows

$$\cos\psi_{(\hat{a},k)} = \cos\psi^{(0)}_{(\hat{a},k)} + \epsilon\cos\psi^{(1)}_{(\hat{a},k)} + \epsilon^2\cos\psi^{(2)}_{(\hat{a},k)} + \epsilon^3\cos\psi^{(3)}_{(\hat{a},k)}, \tag{57}$$

where

$$\begin{aligned}
\cos\psi^{(0)}_{(\hat{a},k)} &= \mathbf{C}_{\hat{a}}\cdot\bar{\ell}_\varnothing,\\
\cos\psi^{(1)}_{(\hat{a},k)} &= (\mathbf{v}\cdot\bar{\ell}_\varnothing)(\mathbf{C}_{\hat{a}}\cdot\bar{\ell}_\varnothing) - \mathbf{C}_{\hat{a}}\cdot\mathbf{v},\\
\cos\psi^{(2)}_{(\hat{a},k)} &= \mathbf{C}_{\hat{a}}\cdot\bar{\ell}^{(2)}_{\rm obs} - \frac{1}{2}(\mathbf{v}\cdot\bar{\ell}_\varnothing)(\mathbf{C}_{\hat{a}}\cdot\mathbf{v}) + (\mathbf{C}_{\hat{a}}\cdot\bar{\ell}_\varnothing)\left[h_{\rm obs} + (\mathbf{v}\cdot\bar{\ell}_\varnothing)^2 - \frac{v^2}{2}\right],\\
\cos\psi^{(3)}_{(\hat{a},k)} &= \mathbf{C}_{\hat{a}}\cdot\bar{\ell}^{(3)}_{\rm obs} + (\mathbf{v}\cdot\bar{\ell}_\varnothing)(\mathbf{C}_{\hat{a}}\cdot\bar{\ell}^{(2)}_{\rm obs}) - (\mathbf{C}_{\hat{a}}\cdot\mathbf{v})\left[2h_{\rm obs} + \frac{1}{2}(\mathbf{v}\cdot\bar{\ell}_\varnothing)^2\right]\\
&\quad + (\mathbf{C}_{\hat{a}}\cdot\bar{\ell}_\varnothing)\left\{(\mathbf{v}\cdot\bar{\ell}_\varnothing)\left[4h_{\rm obs} + (\mathbf{v}\cdot\bar{\ell}_\varnothing)^2 - \frac{v^2}{2}\right] + \mathbf{v}\cdot\bar{\ell}^{(2)}_{\rm obs}\right\}\\
&= \mathbf{C}_{\hat{a}}\cdot\bar{\ell}^{(3)}_{\rm obs} + (\mathbf{v}\cdot\bar{\ell}_\varnothing)\cos\psi^{(2)}_{(\hat{a},k)} + 2h_{\rm obs}\cos\psi^{(1)}_{(\hat{a},k)} + (\mathbf{C}_{\hat{a}}\cdot\bar{\ell}_\varnothing)[h_{\rm obs}(\mathbf{v}\cdot\bar{\ell}_\varnothing) + \mathbf{v}\cdot\bar{\ell}^{(2)}_{\rm obs}],
\end{aligned} \tag{58}$$

with $h_{\rm obs} = GM/r_{\rm obs}$ and $\bar{\ell}_{\rm obs} = \bar{\ell}_\varnothing + \epsilon^2\bar{\ell}^{(2)}_{\rm obs} + \epsilon^3\bar{\ell}^{(3)}_{\rm obs}$, i.e.,

$$\bar{\ell}^a_{\rm obs} = \bar{\ell}^a_\varnothing - GM\epsilon^2\left[\frac{\bar{\ell}^a_\varnothing}{r_{\rm obs}} - 2\frac{d^a}{d^2}\left(\frac{r_*-r_{\rm obs}}{|\mathbf{x}_*-\mathbf{x}_{\rm obs}|} - (\mathbf{n}_{\rm obs}\cdot\bar{\ell}_\varnothing)\right)\right] - 2GM\epsilon^3\left\{\left(\frac{1}{|\mathbf{x}_*-\mathbf{x}_{\rm obs}|}\ln\left[\frac{r_*+(\mathbf{r}_*\cdot\bar{\ell}_\varnothing)}{r_{\rm obs}+(\mathbf{r}_{\rm obs}\cdot\bar{\ell}_\varnothing)}\right] - \frac{2}{r_{\rm obs}}\right)d^a_v + \frac{r_* r_{\rm obs}}{d^2|\mathbf{x}_*-\mathbf{x}_{\rm obs}|}\left[d^a_v - 2\frac{d^a}{d^2}(\tilde{\mathbf{v}}\cdot\mathbf{d})\right](\mathbf{n}_*\cdot\bar{\ell}_\varnothing - \mathbf{n}_{\rm obs}\cdot\bar{\ell}_\varnothing) - \frac{d^a}{d^2}\left[(\tilde{\mathbf{v}}\cdot\bar{\ell}_\varnothing)(\mathbf{n}_{\rm obs}\cdot\bar{\ell}_\varnothing) - \frac{\tilde{\mathbf{v}}\cdot\mathbf{d}}{r_{\rm obs}}\right]\right\}, \tag{59}$$

where we have used the relation

$$\sigma_* = |\mathbf{x}_*-\mathbf{x}_{\rm obs}| + \epsilon^2[1+\epsilon(\tilde{\mathbf{v}}\cdot\bar{\ell}_\varnothing)]H(x^a_*) + GM\epsilon^3\frac{|\mathbf{x}_*-\mathbf{x}_{\rm obs}|}{r_*+(\mathbf{r}_*\cdot\bar{\ell}_\varnothing)}\left[\left(1+\frac{r_*-r_{\rm obs}}{|\mathbf{x}_*-\mathbf{x}_{\rm obs}|}\right)\frac{\tilde{\mathbf{v}}\cdot\mathbf{d}}{r_{\rm obs}+(\mathbf{r}_{\rm obs}\cdot\bar{\ell}_\varnothing)} - \tilde{\mathbf{v}}\cdot\bar{\ell}_\varnothing\right] + O(\epsilon^4). \tag{60}$$

IV. LINKING THE ASTROMETRIC OBSERVABLE TO THE STARS: THE LINEARIZED OBSERVATION EQUATIONS FOR GAIA

Repeated observations of the same objects from different satellite orientations and at different times allows to estimate their angular positions, parallaxes, and proper motions, i.e., the actual realization of an absolute reference frame. This process is conventionally called Astrometric Sphere Reconstruction. From a mathematical point of view, these observations translate into a large number of equations, linearized with respect to the unknown parameters around known initial values, whose solution in the least-squares sense eventually provides the catalog with its errors, and determines the Gaia reference frame.

In principle, the $\hat{a}$-th direction cosine turns out to be a function of the spatial position x^a_* of the star (or, equivalently, its astrometric parameters) and the satellite's attitude represented by the parameters σ_i, i.e.,

$$\cos\psi_{(\hat{a},k)}|_{\sigma=0} = f_{\hat{a}}(x^i_*,\sigma_i) = f^{(0)}_{\hat{a}} + \epsilon f^{(1)}_{\hat{a}} + \epsilon^2 f^{(2)}_{\hat{a}} + \epsilon^3 f^{(3)}_{\hat{a}}, \tag{61}$$

where, according to equations (58), we define:

$$\begin{aligned}
f^{(0)}_{\hat{a}} &= \mathbf{C}_{\hat{a}}\cdot\bar{\ell}_{\varnothing},\\
f^{(1)}_{\hat{a}} &= (\mathbf{v}\cdot\bar{\ell}_{\varnothing})f^{(0)}_{\hat{a}} - \mathbf{C}_{\hat{a}}\cdot\mathbf{v},\\
f^{(2)}_{\hat{a}} &= \mathbf{C}_{\hat{a}}\cdot\bar{\ell}^{(2)}_{\rm obs} + \frac{1}{2}(\mathbf{v}\cdot\bar{\ell}_{\varnothing})f^{(1)}_{\hat{a}}\\
&\quad + f^{(0)}_{\hat{a}}\left[h_{\rm obs} + \frac{1}{2}(\mathbf{v}\cdot\bar{\ell}_{\varnothing})^2 - \frac{v^2}{2}\right],\\
f^{(3)}_{\hat{a}} &= \mathbf{C}_{\hat{a}}\cdot\bar{\ell}^{(3)}_{\rm obs} + (\mathbf{v}\cdot\bar{\ell}_{\varnothing})f^{(2)}_{\hat{a}} + 2h_{\rm obs}f^{(1)}_{\hat{a}}\\
&\quad + f^{(0)}_{\hat{a}}[h_{\rm obs}(\mathbf{v}\cdot\bar{\ell}_{\varnothing}) + \mathbf{v}\cdot\bar{\ell}^{(2)}_{\rm obs}].
\end{aligned} \tag{62}$$

Our task is to make the function f explicit by exploiting the RAMOD/IAU astrometric solution in order to provide a stellar catalogue consistent with the precepts of general relativity, which is also suitable for the validation of the baseline relativistic model for Gaia.

Since Gaia collects a large number of observations, a large overdetermined system is produced that can be linearized around a given starting point x^i_o. Then, in order to determine the unknowns, we have to consider the solution of a linear system of equations such as

$$\mathbf{b} = \mathbf{A}\delta\mathbf{x} \tag{63}$$

where $\mathbf{b} = \{-\sin\phi_j\delta\phi^j\}^T$ $(j = 1,\ldots,n_{\rm obs})$, $\delta\mathbf{x} = \mathbf{x}_{\rm un} - \mathbf{x}_o$ is the unknowns vector, and $\mathbf{A}$ is the $n_{\rm un}\times n_{\rm obs}$ design matrix of the system whose coefficients are $a_{ji} = \partial f/\partial x^i$.

The variation of (61) with respect to any parameters p_i is

$$\delta(\cos\psi_{(\hat{a},k)}|_{\sigma=0}) = \sum_j \frac{\partial f_{\hat{a}}(p_i)}{\partial p_j}\delta p_j, \tag{64}$$

which is easily computed taking into account that

$$\frac{\partial\bar{\ell}^i_{\varnothing}}{\partial x^j_*} = \frac{\delta^{ij} - \bar{\ell}^i_{\varnothing}\bar{\ell}^j_{\varnothing}}{|\mathbf{x}_* - \mathbf{x}_{\rm obs}|} \equiv \frac{P(\bar{\ell}_{\varnothing})^{ij}}{|\mathbf{x}_* - \mathbf{x}_{\rm obs}|}, \tag{65}$$

$$\frac{\partial|\mathbf{x}_* - \mathbf{x}_{\rm obs}|}{\partial x^j_*} = \bar{\ell}^j_{\varnothing}, \qquad \frac{\partial r_*}{\partial x^j_*} = n^j_*, \tag{66}$$

so that

$$\frac{\partial(\mathbf{r}_*\cdot\bar{\ell}_{\varnothing})}{\partial x^j_*} = \bar{\ell}^j_{\varnothing} + \frac{P(\bar{\ell}_{\varnothing})^{ij}r_{*i}}{|\mathbf{x}_* - \mathbf{x}_{\rm obs}|} = \bar{\ell}^j_{\varnothing} + \frac{r^j_* - \bar{\ell}^j_{\varnothing}(\mathbf{r}_*\cdot\bar{\ell}_{\varnothing})}{|\mathbf{x}_* - \mathbf{x}_{\rm obs}|}, \tag{67}$$

and

$$\frac{\partial(\mathbf{v}\cdot\bar{\ell}_{\varnothing})}{\partial x^j_*} = \frac{P(\bar{\ell}_{\varnothing})^{ij}v_i}{|\mathbf{x}_* - \mathbf{x}_{\rm obs}|} = \frac{v^j - \bar{\ell}^j_{\varnothing}(\mathbf{v}\cdot\bar{\ell}_{\varnothing})}{|\mathbf{x}_* - \mathbf{x}_{\rm obs}|}, \tag{68}$$

$$\frac{\partial(\mathbf{C}_{\hat{a}}\cdot\bar{\ell}_{\varnothing})}{\partial x^j_*} = \frac{P(\bar{\ell}_{\varnothing})^{ij}C_{\hat{a}i}}{|\mathbf{x}_* - \mathbf{x}_{\rm obs}|} = \frac{C^j_{\hat{a}} - (\mathbf{C}_{\hat{a}}\cdot\bar{\ell}_{\varnothing})\bar{\ell}^j_{\varnothing}}{|\mathbf{x}_* - \mathbf{x}_{\rm obs}|}, \tag{69}$$

$$\frac{\partial(\mathbf{r}_{\rm obs}\cdot\bar{\ell}_{\varnothing})}{\partial x^j_*} = \frac{d^j}{|\mathbf{x}_* - \mathbf{x}_{\rm obs}|}, \tag{70}$$

$$\frac{\partial d^i}{\partial x^j_*} = -\frac{1}{|\mathbf{x}_* - \mathbf{x}_{\rm obs}|}[\bar{\ell}^i_{\varnothing}d^j + (\mathbf{r}_{\rm obs}\cdot\bar{\ell}_{\varnothing})P(\bar{\ell}_{\varnothing})^{ij}], \tag{71}$$

$$\frac{\partial d}{\partial x^j_*} = -\frac{\mathbf{r}_{\rm obs}\cdot\bar{\ell}_{\varnothing}}{|\mathbf{x}_* - \mathbf{x}_{\rm obs}|}\frac{d^j}{d}, \tag{72}$$

$$\frac{\partial(\tilde{\mathbf{v}}\cdot\mathbf{d})}{\partial x^j_*} = -\frac{(\tilde{\mathbf{v}}\cdot\bar{\ell}_{\varnothing})d^j + (\mathbf{r}_{\rm obs}\cdot\bar{\ell}_{\varnothing})d^j_v}{|\mathbf{x}_* - \mathbf{x}_{\rm obs}|}, \tag{73}$$

$$\frac{\partial(\tilde{\mathbf{v}}\cdot\bar{\ell}_{\varnothing})}{\partial x^j_*} = \frac{d^j_v}{|\mathbf{x}_* - \mathbf{x}_{\rm obs}|}, \tag{74}$$

$$\frac{\partial d^i_v}{\partial x^j_*} = -\frac{1}{|\mathbf{x}_* - \mathbf{x}_{\rm obs}|}[\bar{\ell}^i_{\varnothing}d^j_v + (\tilde{\mathbf{v}}\cdot\bar{\ell}_{\varnothing})P(\bar{\ell}_{\varnothing})^{ij}]. \tag{75}$$

The variations with respect to the attitude parameters is straightforward. We list them in Appendix C.

Actually, each Gaia observation can be translated in the measurement of an abscissa on the $\{x, y\}$ focal plane which can be modeled as a function $f(x_*, x_C, x_I, x_G)$ of the stellar coordinates x^i_*, as well as of those of the satellite attitude x^i_C, instrumental x^i_I, and of another kind called global x^i_G.

Moreover, the attitude reconstruction requires the inclusion of a certain number of across-scan measurements, namely those of the coordinate orthogonal to the same plane.

Then, the actual observables of Gaia are:

$$\cos\phi = \frac{\cos\psi_{(\hat{1},k)}}{\sqrt{1-\cos^2\psi_{(\hat{3},k)}}} = \cos\phi^{(0)} + \epsilon\cos\phi^{(1)} + \epsilon^2\cos\phi^{(2)} + \epsilon^3\cos\phi^{(3)} \quad (76)$$

$$\sin\zeta = \cos\psi_{(\hat{3},k)} = \cos\psi^{(0)}_{(\hat{3},k)} + \epsilon\cos\psi^{(1)}_{(\hat{3},k)} + \epsilon^2\cos\psi^{(2)}_{(\hat{3},k)} + \epsilon^3\cos\psi^{(3)}_{(\hat{3},k)} \quad (77)$$

Let us consider the variation of the observable $\cos\phi$ with respect to the parameters p_i as

$$\delta\cos\phi = \sum_k \frac{\partial\cos\phi(p_i)}{\partial p_k}\delta p_k, \quad (78)$$

The approximations of the across scan measurement are directly given by (58) in the case $\hat{a} = 3$, while those along the scan have the following expressions:

$$\cos\phi^{(0)} = \frac{f^{(0)}_{\hat{1}}}{\sqrt{1-(f^{(0)}_{\hat{3}})^2}},$$

$$\frac{\cos\phi^{(1)}}{\cos\phi^{(0)}} = \frac{f^{(1)}_{\hat{1}}}{f^{(0)}_{\hat{1}}} + \cos^2\phi^{(0)}\frac{f^{(0)}_{\hat{3}}f^{(1)}_{\hat{3}}}{(f^{(0)}_{\hat{1}})^2},$$

$$\frac{\cos\phi^{(2)}}{\cos\phi^{(0)}} = \frac{f^{(2)}_{\hat{1}}}{f^{(0)}_{\hat{1}}} + \cos^2\phi^{(0)}\frac{f^{(0)}_{\hat{3}}}{(f^{(0)}_{\hat{1}})^3}(f^{(1)}_{\hat{1}}f^{(1)}_{\hat{3}} + f^{(0)}_{\hat{1}}f^{(2)}_{\hat{3}}) + \cos^4\phi^{(0)}\frac{(f^{(1)}_{\hat{3}})^2}{2(f^{(0)}_{\hat{1}})^4}(1+2(f^{(0)}_{\hat{3}})^2),$$

$$\frac{\cos\phi^{(3)}}{\cos\phi^{(0)}} = \frac{f^{(3)}_{\hat{1}}}{f^{(0)}_{\hat{1}}} + \cos^2\phi^{(0)}\frac{f^{(0)}_{\hat{3}}}{(f^{(0)}_{\hat{1}})^3}(f^{(2)}_{\hat{1}}f^{(1)}_{\hat{3}} + f^{(1)}_{\hat{1}}f^{(2)}_{\hat{3}} + f^{(0)}_{\hat{1}}f^{(3)}_{\hat{3}}) + \cos^4\phi^{(0)}\frac{f^{(1)}_{\hat{3}}}{2(f^{(0)}_{\hat{1}})^5}(1+2(f^{(0)}_{\hat{3}})^2)(2f^{(0)}_{\hat{1}}f^{(2)}_{\hat{3}} + f^{(1)}_{\hat{1}}f^{(1)}_{\hat{3}}) + \cos^6\phi^{(0)}\frac{f^{(0)}_{\hat{3}}(f^{(1)}_{\hat{3}})^3}{2(f^{(0)}_{\hat{1}})^6}(3+2(f^{(0)}_{\hat{3}})^2). \quad (79)$$

Finally, using the relationships listed in Appendix D, from Eq. (62) we find that the derivatives with respect to the coordinates x^j_* of the star are

$$\frac{\partial f^{(0)}_{\hat{a}}}{\partial x^j_*} = \frac{C^j_{\hat{a}} - f^{(0)}_{\hat{a}}\bar{\ell}^j_{\varnothing}}{|\mathbf{x}_* - \mathbf{x}_{\rm obs}|},$$

$$\frac{\partial f^{(1)}_{\hat{a}}}{\partial x^j_*} = \frac{v^j - \bar{\ell}^j_{\varnothing}(\mathbf{v}\cdot\bar{\ell}_{\varnothing})}{|\mathbf{x}_* - \mathbf{x}_{\rm obs}|}f^{(0)}_{\hat{a}} + (\mathbf{v}\cdot\bar{\ell}_{\varnothing})\frac{\partial f^{(0)}_{\hat{a}}}{\partial x^j_*},$$

$$\frac{\partial f^{(2)}_{\hat{a}}}{\partial x^j_*} = \mathbf{C}_{\hat{a}}\cdot\frac{\partial\bar{\ell}^{(2)}_{\rm obs}}{\partial x^j_*} + \frac{1}{2}[f^{(1)}_{\hat{a}} + 3(\mathbf{v}\cdot\bar{\ell}_{\varnothing})f^{(0)}_{\hat{a}}]\frac{v^j - \bar{\ell}^j_{\varnothing}(\mathbf{v}\cdot\bar{\ell}_{\varnothing})}{|\mathbf{x}_* - \mathbf{x}_{\rm obs}|} + \left[h_{\rm obs} + (\mathbf{v}\cdot\bar{\ell}_{\varnothing})^2 - \frac{v^2}{2}\right]\frac{\partial f^{(0)}_{\hat{a}}}{\partial x^j_*},$$

$$\frac{\partial f^{(3)}_{\hat{a}}}{\partial x^j_*} = \mathbf{C}_{\hat{a}}\cdot\frac{\partial\bar{\ell}^{(3)}_{\rm obs}}{\partial x^j_*} + (\mathbf{v}\cdot\bar{\ell}_{\varnothing})\frac{\partial f^{(2)}_{\hat{a}}}{\partial x^j_*} + (3h_{\rm obs}f^{(0)}_{\hat{a}} + f^{(2)}_{\hat{a}})\frac{v^j - \bar{\ell}^j_{\varnothing}(\mathbf{v}\cdot\bar{\ell}_{\varnothing})}{|\mathbf{x}_* - \mathbf{x}_{\rm obs}|} + [3h_{\rm obs}(\mathbf{v}\cdot\bar{\ell}_{\varnothing}) + \mathbf{v}\cdot\bar{\ell}^{(2)}_{\rm obs}]\frac{\partial f^{(0)}_{\hat{a}}}{\partial x^j_*} + f^{(0)}_{\hat{a}}\left(\mathbf{v}\cdot\frac{\partial\bar{\ell}^{(2)}_{\rm obs}}{\partial x^j_*}\right), \quad (80)$$

where (in units of $GM_{(a)}$, dropping the summation symbol and the subscript (a), for simplicity)

$$\frac{\partial \bar{\ell}^{(2)i}_{\rm obs}}{\partial x^j_*} = -\frac{2}{d^2}\frac{r_*-r_{\rm obs}}{|\mathbf{x}_*-\mathbf{x}_{\rm obs}|^2}\left[d^i\bar{\ell}^j_\varnothing+\bar{\ell}^i_\varnothing d^j+\left(P(\bar{\ell}_\varnothing)^{ij}-2\frac{d^id^j}{d^2}\right)(\mathbf{r}_{\rm obs}\cdot\bar{\ell}_\varnothing)\right]+\frac{2}{d^2}\frac{r_{\rm obs}}{|\mathbf{x}_*-\mathbf{x}_{\rm obs}|}\left(P(\bar{\ell}_\varnothing)^{ij}-2\frac{d^id^j}{d^2}\right)$$
$$+\frac{2}{d^2}\frac{d^in^j_*}{|\mathbf{x}_*-\mathbf{x}_{\rm obs}|}+\frac{1}{|\mathbf{x}_*-\mathbf{x}_{\rm obs}|}\left[-3P(\bar{\ell}_\varnothing)^{ij}+2\frac{d^id^j}{d^2}+2(\mathbf{r}_{\rm obs}\cdot\bar{\ell}_\varnothing)\frac{\bar{\ell}^i_\varnothing d^j}{d^2}\right]\frac{1}{r_{\rm obs}},$$

$$\frac{\partial \bar{\ell}^{(3)i}_{\rm obs}}{\partial x^j_*} = \frac{2}{|\mathbf{x}_*-\mathbf{x}_{\rm obs}|^2}[d^i_v\bar{\ell}^j_\varnothing+\bar{\ell}^i_\varnothing d^j_v+(\tilde{\mathbf{v}}\cdot\bar{\ell}_\varnothing)P(\bar{\ell}_\varnothing)^{ij}]\ln\left[\frac{r_*+(\mathbf{r}_*\cdot\bar{\ell}_\varnothing)}{r_{\rm obs}+(\mathbf{r}_{\rm obs}\cdot\bar{\ell}_\varnothing)}\right]$$
$$-2\frac{P(\bar{\ell}_\varnothing)^{ij}}{|\mathbf{x}_*-\mathbf{x}_{\rm obs}|}\left[(\tilde{\mathbf{v}}\cdot\bar{\ell}_\varnothing)\left(\frac{1}{r_{\rm obs}}+\frac{r_*-r_{\rm obs}}{|\mathbf{x}_*-\mathbf{x}_{\rm obs}|}\frac{\mathbf{r}_{\rm obs}\cdot\bar{\ell}_\varnothing}{d^2}\right)-\frac{\tilde{\mathbf{v}}\cdot\mathbf{d}}{d^2}(\mathbf{r}_{\rm obs}\cdot\bar{\ell}_\varnothing)\left(\frac{1}{r_{\rm obs}}-2\frac{r_{\rm obs}}{d^2}+2\frac{r_*-r_{\rm obs}}{|\mathbf{x}_*-\mathbf{x}_{\rm obs}|}\frac{\mathbf{r}_{\rm obs}\cdot\bar{\ell}_\varnothing}{d^2}\right)\right]$$
$$+2\frac{d^i_v}{|\mathbf{x}_*-\mathbf{x}_{\rm obs}|}\left\{n_{*m}\left[\delta^{mj}\frac{\mathbf{r}_{\rm obs}\cdot\bar{\ell}_\varnothing}{b^2}-\frac{1}{1+(\mathbf{n}_*\cdot\bar{\ell}_\varnothing)}\left(\frac{P(\bar{\ell}_\varnothing)^{mj}}{|\mathbf{x}_*-\mathbf{x}_{\rm obs}|}+\frac{\delta^{mj}}{r_*}\right)\right]-\bar{\ell}^j_\varnothing\left(\frac{1}{r_*+(\mathbf{r}_*\cdot\bar{\ell}_\varnothing)}+\frac{r_*-r_{\rm obs}}{|\mathbf{x}_*-\mathbf{x}_{\rm obs}|}\frac{\mathbf{r}_{\rm obs}\cdot\bar{\ell}_\varnothing}{d^2}\right)\right.$$
$$\left.+\frac{d^j}{d^2}\left[\frac{r_*-\mathbf{r}_{\rm obs}\cdot\bar{\ell}_\varnothing}{|\mathbf{x}_*-\mathbf{x}_{\rm obs}|}-2\frac{r_{\rm obs}(\mathbf{r}_{\rm obs}\cdot\bar{\ell}_\varnothing)}{d^2}\left(1-\frac{r_*-r_{\rm obs}}{|\mathbf{x}_*-\mathbf{x}_{\rm obs}|}(\mathbf{n}_{\rm obs}\cdot\bar{\ell}_\varnothing)\right)\right]\right\}$$
$$-2\frac{\bar{\ell}^i_\varnothing}{r_{\rm obs}|\mathbf{x}_*-\mathbf{x}_{\rm obs}|}\left\{\left(d^j_v-2d^j\frac{\tilde{\mathbf{v}}\cdot\mathbf{d}}{d^2}\right)\left[1+\frac{r_{\rm obs}(\mathbf{r}_{\rm obs}\cdot\bar{\ell}_\varnothing)}{d^2}\left(\frac{r_*-r_{\rm obs}}{|\mathbf{x}_*-\mathbf{x}_{\rm obs}|}-(\mathbf{n}_{\rm obs}\cdot\bar{\ell}_\varnothing)\right)\right]+\frac{d^j}{d^2}[2(\tilde{\mathbf{v}}\cdot\mathbf{d})+(\tilde{\mathbf{v}}\cdot\mathbf{r}_{\rm obs})]\right\}$$
$$+4\frac{d^i}{d^4|\mathbf{x}_*-\mathbf{x}_{\rm obs}|}\left\{(\tilde{\mathbf{v}}\cdot\mathbf{d})(\mathbf{r}_{\rm obs}\cdot\bar{\ell}_\varnothing)\left(\bar{\ell}^j_\varnothing\frac{r_*-r_{\rm obs}}{|\mathbf{x}_*-\mathbf{x}_{\rm obs}|}-n^j_*-\frac{d^j}{r_{\rm obs}}\right)\right.$$
$$\left.+\left[(\mathbf{r}_{\rm obs}\cdot\bar{\ell}_\varnothing)^2d^j_v-4d^jr^2_{\rm obs}\frac{\tilde{\mathbf{v}}\cdot\mathbf{d}}{d^2}\right]\left(\frac{r_*-r_{\rm obs}}{|\mathbf{x}_*-\mathbf{x}_{\rm obs}|}-(\mathbf{n}_{\rm obs}\cdot\bar{\ell}_\varnothing)\right)+d^j\frac{r_*-r_{\rm obs}}{|\mathbf{x}_*-\mathbf{x}_{\rm obs}|}[2(\tilde{\mathbf{v}}\cdot\mathbf{d})+(\tilde{\mathbf{v}}\cdot\mathbf{r}_{\rm obs})]\right\}. \quad (81)$$

Once the system is solved, in order to transform the BCRS coordinates to those of the astrometric catalogue (α,δ) at a given epoch t_0, it is enough to apply the well-known transformations

$$\mathbf{x}_* = \frac{1}{\varpi}(\cos\alpha\cos\delta, \sin\alpha\cos\delta, \sin\delta), \quad (82)$$

where ϖ is the parallax, while the proper motion can be deduced by a Taylor expansion of the first order

$$\alpha(t) = \alpha(t_0)+\mu_\alpha(t-t_0)+O(\Delta t^2), \quad (83)$$

$$\delta(t) = \delta(t_0)+\mu_\delta(t-t_0)+O(\Delta t^2). \quad (84)$$

V. NUMERICAL TESTS ON THE INTRINSIC CONSISTENCY OF THE ASTROMETRIC MODEL

The problem of the analytical comparison of the static RAMOD solution (RAMOD3s) and the above models with the others available in the literature has been already dealt with in previous papers [25,26]. Nonetheless, the present arrangement of the RAMOD formulas (RAMOD4a) with the inclusion of the gravitational source velocity contributions has been conceived in the mindset of an application of this astrometric model to Gaia, and in particular to its implementation in the GSR pipeline. In this context it is mandatory to provide convincing proofs of the consistency and of the reliability of the formulas also from a numerical point of view, before proceeding with their actual implementation.

In this regard, two kinds of numerical tests have been performed to check the theoretical algorithms of this paper:

(1) the comparison of the predicted Gaia observable with the one obtained by the GREM model (Klioner, 2003) used by the AGIS sphere reconstruction;
(2) the estimation of the astrometric unknowns of some selected stars in a Gaia-like case specifically designed to show the numerical differences between the two astrometric models.

Both of these two different tests are needed to guarantee the correctness of the resulting linearized observation equations. The first one can show the differences between GREM and RAMOD4a in the computation of the Along-scan (AL) and Across-scan (AC) Gaia measurements, thus testing the known terms side of the observations equations. The second one, instead, requires the computation of the coefficients of the linearized equation through Eqs. (76)–(81), and therefore represents a test of the complete equation, at least for its purely astrometric part.

For the known-terms test, we used samples from the RDS-7-F Gaia simulated data (the same data set used for testing AGIS), which provided the coordinates of the stars, the ephemerides of the Solar System bodies, the position and velocity of the satellite, and the time of each observation in the BCRS. These data are sufficient to compute

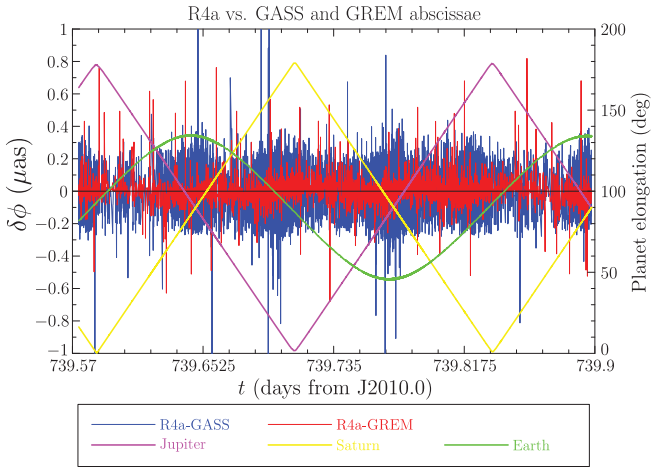

FIG. 1. Differences between the AL measurements as predicted by RAMOD4a and GREM, computed with the both the older and less accurate version used in the DPAC software that produced the simulated dataset (GASS, in blue) and with the newer version (GREM, in red). In the case of GASS there are very few observations with differences up to 10 μas which are not shown here because the scale was cropped to ± 1 μas. The plot also shows the elongation of the main perturbing bodies, reported on the right axis, from the observed star. These results refer to an 8-hours sample of observations around day 740 of the simulation.

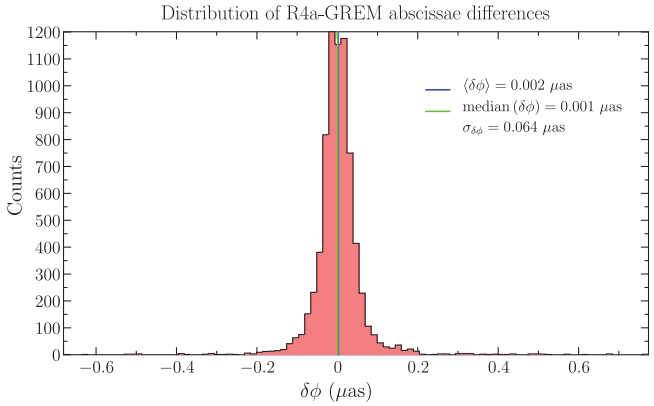

FIG. 2. Histogram of the differences between the AL measurements as predicted by RAMOD4a and GREM, computed with the latest implementation of the DPAC software used by the AGIS pipeline. These results refer to the same 8-hours sample of the previous plot.

the AL and AC measurements with the RAMOD4a model. In this case, the numerical evaluation was done with MAPLE, while the same data was used to compute also the corresponding values for GREM using the standard DPAC software.

The results show that the differences between these two models is always well below the μas level, thus proving their equivalence also from the numerical point of view at the accuracy level required for Gaia. In Fig. 1 we took an example in which Gaia is observing close to Jupiter, and thus in the most challenging conditions from the point of view of a relativistic astrometric model.

The simulated dataset provided also the estimation of the so-called *field angles* η and ζ. These two quantities are respectively the along-scan and across-scan angles taken from the axis of the Field of View (FoV), and therefore they give the same Gaia measurements of above since $\phi = \eta + \Gamma/2$. Although not strictly necessary, we decided to compare also these values with the RAMOD4a estimations. Indeed, it was known that in the simulation they had been computed using an older, and less accurate implementation of GREM. We therefore used these data to verify this known issue. Fig. 1 is a plot of the differences of RAMOD4a with the old GREM in comparison with those of the new one previously shown, in which it can be seen that the former are sistematically larger, as expected.

The results on the former differences, namely those between RAMOD4a and the newer GREM, are shown also in the histogram form of Fig. 2. In this case the average and the median of these differences are sensible to a systematic difference between these two models in a global sense, which is of the order of a nano-arcsecond.

The goal of the second test was to have a numerical evaluation of RAMOD4a that strictly regarded the accuracy of this relativistic model with respect to GREM. In other words, because of the goal of this paper, we purposedly avoided any possible different source of numerical errors. In particular

(1) it was supposed to have infinitely precise measurements, thus avoiding to perturb the known terms with a random noise that could mimick the Gaia measurement error;
(2) in the real case, as recalled in Eqs. (63), (82), (83) the values used as a starting point for the linearized observation equation are affected by the so-called *catalog errors*, which introduces further approximations since the expansion neglects terms of the second order and above. These numerical approximations are zeroed if, as it is always possible with simulated data, one uses the true values instead of the catalog ones for the starting point of the expansion.

With these two assumptions, and if $\phi_{\rm obs}$ and $\phi_{\rm calc}$ were computed with the same astrometric model, the known term would be identically zero. The expected solution would therefore be zero, except for the standard round-off errors of the algorithm used to solve the equation system.

In our case, however, we are in a sort of "double blind" condition, and the known term is of the order of the differences between the GREM model, used to compute $\phi_{\rm obs}$, and the RAMOD4a, used to compute $\phi_{\rm calc}$. The residuals will thus be affected by such differences, in addition to the previously mentioned round-off errors, and the two models can be considered compatible at the Gaia level of accuracy only if the solution is at least at the sub-μas level.

TABLE I. Results of the single-star reconstruction for the four chosen stars. The astrometric parameters solutions are expressed in μas and μas/yr.

Star	α (deg)	δ (deg)	$d\varpi$	$d\alpha\cos\delta$	$d\delta$	$d\mu_\alpha\cos\delta$	$d\mu_\delta$
1	28.805	9.498	−0.008	−0.109	−0.059	−0.018	−0.021
2	28.722	10.799	−0.017	0.082	−0.153	−0.024	−0.024
3	28.955	10.452	0.009	−0.138	−0.034	−0.032	0.009
4	207.512	−8.528	0.020	−0.002	−0.004	−0.007	−0.017

The limited performances of MAPLE with respect to the needed numerical calculations prevent a complete sphere solution with a large number of stars. However, given the goal of this section, that is for having a test that can prove the reliability of the calculations and the numerical accuracy of RAMOD4a with respect to GREM in the sense mentioned above, it is sufficient to use a very limited number of stars.

We thus decided to limit the test to 4 stars, selected among those which are mostly affected by the influence of Jupiter and Saturn. When only the astrometric parameters are reconstructed, each star can be treated independently from each other. This implies that each star produces a system of ∼700 linear equations which has to be solved in the least-squares sense, namely one has to invert the resulting 5×5 normal matrix to find the solution. The results are reported in Table I, which shows that the residuals are at the expected level.

In the context of the Gaia astrometric sphere reconstruction discussed at the beginning of the previous section, a complete verification demands the reduction of a full sphere and the estimation of both astrometric and attitude parameters. The size of such a task requires a fully optimized implementation of the formulas above on parallel computers in a high-performance computing environment. This is under development as part of the DPAC-GSR pipeline [11] and will be reported in a forthcoming publication [10].

VI. CONCLUDING REMARKS

Missions like Gaia demand the proper treatment of gravity when compiling stellar catalogues to microarcsecond accuracy. High-precision measurements, by demanding suitable relativistic modeling, need to be validated. In this regard, it is of capital importance to allow the existence of different and cross-checked models which exploit different solutions to interpret the same experimental data. Indeed, the main Solar System curvature perturbation, e.g. of the Sun, amounts approximately to 100 μ-as, which will cause the individual parallaxes to quickly degrade beyond 1 kpc, while completely invalidating the most accurate calibration of primary distance calibrators. This alone is sufficient reason for making a theoretical and numerical comparison of the existing approaches a necessity and set the scientific case for further developments and applications.

The realization of the relativistic celestial sphere for the Milky Way is a scientific validation of the absolute parallaxes and proper motions in Gaia data and in their ensuing scientific exploitation. Reaching $10-20$ μas accuracy on the individual parallax and annual proper motions for bright stars ($V < 16$) is also key to performing what is possibly the largest GR experiment ever attempted from space: given the number of celestial objects (a real Galilean method applied on the sky) and directions involved (the whole celestial sphere), one billion light deflection measurements represent the largest experiment in general relativity ever made with astrometric methods since 1919. Moreover, using a fully GR astrometric model will allow new tests of GR predictions and a full probe of the Milky Way's (outer) halo (mass content and distribution) so that we can compare the prediction of ΛCDM models on a local scale. The GR correct picture of the Milky Way, as well as the correct modeling of the measurements from within the Solar System, is the only way to ensure a strong and coherent laboratory against which fundamental physics and the current formation/evolution model can be completely tested.

But all the above cannot be claimed without carefully implementing, checking, and testing the basic starting steps as shown in this paper. In fact, the actual Gaia relativistic modeling for the inverse light-tracing represents the first stage toward the correct approach when increasing the level of the measurement precision, requiring us to refine consistently the perturbation terms of the metric of the solar system, the solutions of the null geodesic, the relativistic attitude, and so on. Preserving the conceptual consistency to GR while extending the complexity of the theoretical approaches to match the high-accuracy observations without a solid test bed for the numerical testing protocol and a detailed comparison between the different methods could be very dangerous for the scientific interpretation of the results and may lead to unnecessary modifications of GR, the current standard theory of gravity.

Relativistic astrometry extends beyond the scope of Gaia: after Gaia, astrometry becomes part of the fundamental physics and, in particular, that of gravitation.

ACKNOWLEDGMENTS

This work has been (partially) funded by ASI under contract Gaia Mission—The Italian Participation to DPAC, 2014-025-R.1.2015. The authors thanks Fernando de Felice for his constant support on the theoretical side, Ummi Abbas and Ronald Drimmel for their helpful comments which improved the text.

During this work, A. Geralico was one year INAF research associate at OATo under Contract No. inaf-816rm.AOO-af-TO. REGISTRO UFFICIALE.I.0000444.25-817 02-2016 (Dr. M. Crosta supervisor).

APPENDIX A: TIME RETARDED CONSIDERATIONS

Consider the following canonical metric [18,29],

$$
\begin{aligned}
h^{00}_{\rm can}(cT,X^i) &= \frac{4G}{c^2}\sum_{l=0}^{\infty}\frac{(-1)^l}{l!}\partial_L\left[\frac{M_L(U)}{R}\right],\\
h^{0i}_{\rm can}(cT,X^i) &= -\frac{4G}{c^3}\sum_{l=1}^{\infty}\frac{(-1)^l}{l!}\left\{\partial_{L-1}\left[\frac{\dot{M}_{iL-1}(U)}{R}\right]\right.\\
&\quad\left.+\frac{l}{l+1}\varepsilon_{iab}\partial_{aL-1}\left[\frac{S_{bL-1}(U)}{R}\right]\right\},\\
h^{ij}_{\rm can}(cT,X^i) &= \frac{4G}{c^4}\sum_{l=2}^{\infty}\frac{(-1)^l}{l!}\left\{\partial_{L-2}\left[\frac{\ddot{M}_{ijL-2}(U)}{R}\right]\right.\\
&\quad\left.+\frac{2l}{l+1}\partial_{aL-2}\left[\frac{\varepsilon_{ab(i}\dot{S}_{j)bL-2}(U)}{R}\right]\right\},
\end{aligned}
\tag{A1}
$$

where the multipole moments are Cartesian symmetric and tracefree (STF) tensors, all of them evaluated at the retarded time $T_{\rm ret}=T-R/c$, $R=\sqrt{\delta_{ij}X^iX^j}$ (the overdot denoting differentiation with respect to $T_{\rm ret}$, and $\partial_L=\partial^l/(\partial X^{a_1}\partial X^{a_2}\ldots\partial X^{a_l})$). The distance R which appears in the local metric (A1) can be written in Lorentz invariant form as [29]

$$
\begin{aligned}
R &= \epsilon|\eta_{\mu\nu}u^\mu(x^\nu-x_0^\nu(t_{\rm ret}))|\\
&= \gamma[r(t_{\rm ret})-\epsilon\tilde{\mathbf{v}}\cdot\mathbf{r}(t_{\rm ret})]\\
&= [r(t)^2+\epsilon^2\gamma^2(\tilde{\mathbf{v}}\cdot\mathbf{r}(t))^2]^{1/2},
\end{aligned}
\tag{A2}
$$

where $\epsilon=1/c$, $r^i(t_{\rm ret})=x^i-x^i(t_{\rm ret})$, $r^i(t)=x^i-x^i(t)$, and $t_{\rm ret}$ the retarded time in the global coordinate system. The latter reads for arbitrary word lines as

$$
t_{\rm ret}(ct,x^i)=t-\epsilon|\mathbf{x}-\mathbf{x}_0(t_{\rm ret})|,
\tag{A3}
$$

which is an implicit relation between $t_{\rm ret}$ and t. In the case of a body in uniform motion, it can be approximated as

$$
\begin{aligned}
t_{\rm ret}(ct,x^i) &\approx t-\epsilon\gamma^2[\epsilon\mathbf{r}(t)\cdot\tilde{\mathbf{v}}+(r(t)^2-\epsilon^2(\mathbf{r}(t)\times\tilde{\mathbf{v}})^2)^{1/2}]\\
&= t-\epsilon r(t)-\epsilon^2\tilde{\mathbf{v}}\cdot\mathbf{r}(t)+O(\epsilon^3),
\end{aligned}
\tag{A4}
$$

which is related to $T_{\rm ret}$ simply by $T_{\rm ret}=\gamma^{-1}(t_{\rm ret}-t_0)$.

Note that the expressions (11) can be obtained using the approximation in [24] performing a Taylor expansion with respect to the time coordinate of the metric coefficient. On the hypersurface corresponding to the time of observation, let us consider $\mathbf{r}^{(a)}=\mathbf{r}_0^{(a)}+\tilde{\mathbf{r}}^{(a)}$, where $\mathbf{r}_0^{(a)}=\{x(t)-x^{(a)}(t),y(t)-y^{(a)}(t),z(t)-z^{(a)}(t)\}$ is the position vector of the photon with respect to the body, but calculated at the time t, and $\tilde{\mathbf{r}}^{(a)}=\{x^{(a)}(t)-x^{(a)}(t'),y^{(a)}(t)-y^{(a)}(t'),z^{(a)}(t)-z^{(a)}(t')\}$ is the difference between the positions of the body at the time t and at the retarded time t'.

The *reduced distance* $r^{(a)}=\sqrt{\delta_{ij}(r_0^i+\tilde{r}^i)(r_0^j+\tilde{r}^j)}+O(h)$ in the metric adopted in [24], namely,

$$
\begin{aligned}
h_{00} &= 2\sum_a\epsilon^2\frac{\mathcal{M}_{(a)}}{r^{(a)}}(1+\mathbf{n}^{(a)}\cdot\tilde{\mathbf{v}}_{(a)})+\mathcal{O}(\epsilon^4),\\
h_{0i} &= -4\sum_a\epsilon^3\frac{\mathcal{M}_{(a)}}{r^{(a)}}\tilde{v}_{i(a)}+\mathcal{O}(\epsilon^5),\\
h_{ij} &= 2\sum_a\epsilon^2\frac{\mathcal{M}_{(a)}}{r^{(a)}}(1+\mathbf{n}^{(a)}\cdot\tilde{\mathbf{v}}_{(a)})\delta_{ij}+\mathcal{O}(\epsilon^4),
\end{aligned}
\tag{A5}
$$

can be approximated on the hypersurface at $t=t_{\rm obs}$ as

$$
r^{(a)}=r_0\left(1+\frac{\mathbf{r}_0\cdot\tilde{\mathbf{r}}}{r_0^2}\right)+\mathcal{O}\left(\frac{\tilde{r}^2}{r_0^2}\right).
\tag{A6}
$$

Then, the final expression for the metric coefficient h_{00} is

$$
h_{00}\simeq\sum_a\epsilon^2\frac{2G\mathcal{M}^{(a)}}{r_0^{(a)}}\left(1+\frac{\mathbf{v}^{(a)}\cdot\mathbf{r}_0^{(a)}}{cr_0^{(a)}}-\frac{\mathbf{r}_0^{(a)}\cdot\tilde{\mathbf{r}}^{(a)}}{(r_0^{(a)})^2}\right).
\tag{A7}
$$

However, we stress that the quantities inside the parentheses are still functions of both the time t and of the retarded time t', that is $\mathbf{v}^{(a)}\equiv\mathbf{v}^{(a)}(t')$, $\mathbf{r}_0^{(a)}\equiv\mathbf{r}_0^{(a)}(t)$ and $\tilde{\mathbf{r}}^{(a)}\equiv\tilde{\mathbf{r}}^{(a)}(t,t')$. The dependence on t' can be avoided with a further Taylor expansion around t:

$$
\tilde{r}^i=\tilde{x}^i(t)-\tilde{x}^i(t-r_0\epsilon)=r_0\epsilon\tilde{v}^i(t)+\frac{1}{2}r_0^2\epsilon^2\tilde{a}^i(t)+\mathcal{O}(\epsilon^3)
$$

$$
\tilde{v}^i(t')=\tilde{v}^i(t)-\tilde{a}^i(t)r_0\epsilon+\mathcal{O}(\epsilon^2).
$$

Inserting these expansions into term (A7), it is straightforward to show that the retarded approximated contributions cancel out in the metric coefficient h_{00} up to the ϵ^3 order.

APPENDIX B: THE EXPRESSION OF LIGHT TRAJECTORY BASIC INTEGRALS

The solutions of the null goedesic are given by Eq. (28), where functions $H(\sigma)$, $H^a(\sigma)$, and $\mathcal{H}^a(\sigma)$, at the lowest order, are

$$
\begin{aligned}
H(\sigma) &= GM[1+\epsilon(\tilde{\mathbf{v}}\cdot\bar{\ell}_\varnothing)]\ln\left[\frac{r+(\mathbf{r}\cdot\bar{\ell}_\varnothing)}{r_{\rm obs}+(\mathbf{r}_{\rm obs}\cdot\bar{\ell}_\varnothing)}\right]+\frac{GM}{r+(\mathbf{r}\cdot\bar{\ell}_\varnothing)}\left[\frac{r-r_{\rm obs}+\sigma}{r_{\rm obs}+(\mathbf{r}_{\rm obs}\cdot\bar{\ell}_\varnothing)}(\tilde{\mathbf{v}}\cdot\mathbf{d})-(\tilde{\mathbf{v}}\cdot\bar{\ell}_\varnothing)\sigma\right]\epsilon+O(\epsilon^2),\\
H^a(\sigma) &= GM\left[\bar{\ell}^a_\varnothing\left(\frac{1}{r}-\frac{1}{r_{\rm obs}}\right)-\frac{d^a}{d^2}(\mathbf{n}\cdot\bar{\ell}_\varnothing-\mathbf{n}_{\rm obs}\cdot\bar{\ell}_\varnothing)\right]+GM\left\{\frac{r_{\rm obs}}{d^2 r}\left[d^a_v-2\frac{d^a}{d^2}(\tilde{\mathbf{v}}\cdot\mathbf{d})\right][r-r_{\rm obs}-(\mathbf{n}_{\rm obs}\cdot\bar{\ell}_\varnothing)\sigma]\right.\\
&\quad\left.+\left[\bar{\ell}^a_\varnothing(\tilde{\mathbf{v}}\cdot\bar{\ell}_\varnothing)-\frac{d^a}{d^2}(\tilde{\mathbf{v}}\cdot\mathbf{r}_{\rm obs})\right]\left(\frac{1}{r}-\frac{1}{r_{\rm obs}}\right)-\bar{\ell}^a_\varnothing\frac{\tilde{\mathbf{v}}\cdot\mathbf{d}}{d^2}(\mathbf{n}\cdot\bar{\ell}_\varnothing-\mathbf{n}_{\rm obs}\cdot\bar{\ell}_\varnothing)\right\}\epsilon+O(\epsilon^2),\\
\mathcal{H}^a(\sigma) &= \bar{\ell}^a_\varnothing[1+\epsilon(\tilde{\mathbf{v}}\cdot\bar{\ell}_\varnothing)]\left[H(\sigma)-\frac{GM}{r_{\rm obs}}\sigma\right]-GM\left[\frac{d^a}{d^2}[1+2\epsilon(\tilde{\mathbf{v}}\cdot\bar{\ell}_\varnothing)]+\epsilon\bar{\ell}^a_\varnothing\frac{\tilde{\mathbf{v}}\cdot\mathbf{d}}{d^2}\right][r-r_{\rm obs}-(\mathbf{n}_{\rm obs}\cdot\bar{\ell}_\varnothing)\sigma]\\
&\quad+\left\{d^a_v H(\sigma)-\frac{r r_{\rm obs}}{d^2}\left[d^a_v-2\frac{d^a}{d^2}(\tilde{\mathbf{v}}\cdot\mathbf{d})\right](\mathbf{n}\cdot\bar{\ell}_\varnothing-\mathbf{n}_{\rm obs}\cdot\bar{\ell}_\varnothing)+\frac{d^a}{d^2 r_{\rm obs}}[(\tilde{\mathbf{v}}\cdot\bar{\ell}_\varnothing)(\mathbf{r}_{\rm obs}\cdot\bar{\ell}_\varnothing)-(\tilde{\mathbf{v}}\cdot\mathbf{d})]\sigma\right\}\epsilon+O(\epsilon^2),
\end{aligned}
\tag{B1}
$$

and

$$
\begin{aligned}
H^t(\sigma) &= -GM\left[(\tilde{\mathbf{v}}\cdot\bar{\ell}_\varnothing)\left(\frac{1}{r}-\frac{1}{r_{\rm obs}}\right)-\frac{\tilde{\mathbf{v}}\cdot\mathbf{d}}{d^2}(\mathbf{n}\cdot\bar{\ell}_\varnothing-\mathbf{n}_{\rm obs}\cdot\bar{\ell}_\varnothing)\right]+O(\epsilon),\\
\mathcal{H}^t(\sigma) &= -(\tilde{\mathbf{v}}\cdot\bar{\ell}_\varnothing)\left(H(\sigma)-\frac{GM}{r_{\rm obs}}\sigma\right)+GM\frac{\tilde{\mathbf{v}}\cdot\mathbf{d}}{d^2}[r-r_{\rm obs}-(\mathbf{n}_{\rm obs}\cdot\bar{\ell}_\varnothing)\sigma]+O(\epsilon),
\end{aligned}
\tag{B2}
$$

Note that $H^t(\sigma)=-\delta_{ab}H^a(\sigma)\tilde{v}^b$ and $\mathcal{H}^t(\sigma)=-\delta_{ab}\mathcal{H}^a(\sigma)\tilde{v}^b$, since $\partial_t h=-\tilde{v}^a\partial_a h$, and

$$
\mathcal{E}(K,u)=1+GM\epsilon^2[1+\epsilon(\tilde{\mathbf{v}}\cdot\bar{\ell}_\varnothing)]\left(\frac{1}{r}-\frac{1}{r_{\rm obs}}\right)-GM\epsilon^3\frac{\tilde{\mathbf{v}}\cdot\mathbf{d}}{d^2}(\mathbf{n}\cdot\bar{\ell}_\varnothing-\mathbf{n}_{\rm obs}\cdot\bar{\ell}_\varnothing)+O(\epsilon^4),
\tag{B3}
$$

being

$$
H^0(\sigma)=-\delta_{ab}\mathcal{H}^a(\sigma)\tilde{v}^b=-GM\left[(\tilde{\mathbf{v}}\cdot\bar{\ell}_\varnothing)\left(\frac{1}{r}-\frac{1}{r_{\rm obs}}\right)-\frac{\tilde{\mathbf{v}}\cdot\mathbf{d}}{d^2}(\mathbf{n}\cdot\bar{\ell}_\varnothing-\mathbf{n}_{\rm obs}\cdot\bar{\ell}_\varnothing)\right].
\tag{B4}
$$

For a mass monopole one gets

$$
\begin{aligned}
H_M(\sigma) &= GM\ln\left[\frac{r+(\mathbf{x}\cdot\bar{\ell}_\varnothing)}{r_{\rm obs}+(\mathbf{x}_{\rm obs}\cdot\bar{\ell}_\varnothing)}\right],\\
H^a_M(\sigma) &= GM\left[\bar{\ell}^a_\varnothing\left(\frac{1}{r}-\frac{1}{r_{\rm obs}}\right)-\frac{d^a}{d^2}\left(\frac{\mathbf{x}\cdot\bar{\ell}_\varnothing}{r}-\frac{\mathbf{x}_{\rm obs}\cdot\bar{\ell}_\varnothing}{r_{\rm obs}}\right)\right],\\
\mathcal{H}^a_M(\sigma) &= \bar{\ell}^a_\varnothing\left[H_M(\sigma)-\frac{GM}{r_{\rm obs}}[(\mathbf{x}\cdot\bar{\ell}_\varnothing)-(\mathbf{x}_{\rm obs}\cdot\bar{\ell}_\varnothing)]\right]-GM\frac{d^a}{d^2}\left[r-r_{\rm obs}-\frac{\mathbf{x}_{\rm obs}\cdot\bar{\ell}_\varnothing}{r_{\rm obs}}[(\mathbf{x}\cdot\bar{\ell}_\varnothing)-(\mathbf{x}_{\rm obs}\cdot\bar{\ell}_\varnothing)]\right],
\end{aligned}
\tag{B5}
$$

where

$$
r=\sqrt{d^2+(\mathbf{x}\cdot\bar{\ell}_\varnothing)^2},\qquad \frac{{\rm d}r}{{\rm d}\sigma}=\frac{\mathbf{x}\cdot\bar{\ell}_\varnothing}{r}.
\tag{B6}
$$

Then, in the case of a static mass monopole, the solutions are

$$
\begin{aligned}
\bar{\ell}^0 &= 0,\\
\bar{\ell}^a-\bar{\ell}^a_{\rm obs} &= -2GM\epsilon^2\left[\frac{1}{2}\left(\frac{1}{r}-\frac{1}{r_{\rm obs}}\right)\bar{\ell}^a_\varnothing+\frac{d^a}{d^2}\left(\frac{\mathbf{x}\cdot\bar{\ell}_\varnothing}{r}-\frac{\mathbf{x}_{\rm obs}\cdot\bar{\ell}_\varnothing}{r_{\rm obs}}\right)\right]+O(\epsilon^4),\\
x^0-x^0_{\rm obs} &= \sigma+\epsilon^2 GM\ln\left[\frac{r+(\mathbf{x}\cdot\bar{\ell}_\varnothing)}{r_{\rm obs}+(\mathbf{x}_{\rm obs}\cdot\bar{\ell}_\varnothing)}\right]+O(\epsilon^4),\\
x^a-x^a_{\rm obs} &= \bar{\ell}^a_{\rm obs}\sigma-2GM\epsilon^2\left\{\frac{1}{2}\left(\ln\left[\frac{r+(\mathbf{x}\cdot\bar{\ell}_\varnothing)}{r_{\rm obs}+(\mathbf{x}_{\rm obs}\cdot\bar{\ell}_\varnothing)}\right]-\frac{1}{r_{\rm obs}}[(\mathbf{x}-\mathbf{x}_{\rm obs})\cdot\bar{\ell}_\varnothing]\right)\bar{\ell}^a_\varnothing+\frac{d^a}{d^2}\left[r-r_{\rm obs}-\frac{\mathbf{x}_{\rm obs}\cdot\bar{\ell}_\varnothing}{r_{\rm obs}}[(\mathbf{x}-\mathbf{x}_{\rm obs})\cdot\bar{\ell}_\varnothing]\right]\right\}\\
&\quad+O(\epsilon^4),
\end{aligned}
\tag{B7}
$$

and

$$\mathcal{E}(K,u) = 1 + GM\epsilon^2\left(\frac{1}{r} - \frac{1}{r_{\rm obs}}\right) + O(\epsilon^4). \tag{B8}$$

APPENDIX C: DERIVATIVES WITH RESPECT TO THE ATTITUDE PARAMETERS σ_i

From Eq. (62), we deduce

$$\begin{aligned}
&\frac{\partial f_{\hat{a}}^{(0)}}{\partial\sigma_j} = \frac{\partial \mathbf{C}_{\hat{a}}}{\partial\sigma_j}\cdot\bar{\ell}_{\varnothing}, \qquad \frac{\partial f_{\hat{a}}^{(1)}}{\partial\sigma_j} = (\mathbf{v}\cdot\bar{\ell}_{\varnothing})\frac{\partial f_{\hat{a}}^{(0)}}{\partial\sigma_j} - \frac{\partial \mathbf{C}_{\hat{a}}}{\partial\sigma_j}\cdot\mathbf{v},\\
&\frac{\partial f_{\hat{a}}^{(2)}}{\partial\sigma_j} = \frac{\partial \mathbf{C}_{\hat{a}}}{\partial\sigma_j}\cdot\bar{\ell}_{\rm obs}^{(2)} + \frac{1}{2}(\mathbf{v}\cdot\bar{\ell}_{\varnothing})\frac{\partial f_{\hat{a}}^{(1)}}{\partial\sigma_j} + \left[h_{\rm obs} + \frac{1}{2}(\mathbf{v}\cdot\bar{\ell}_{\varnothing})^2 - \frac{v^2}{2}\right]\frac{\partial f_{\hat{a}}^{(0)}}{\partial\sigma_j},\\
&\frac{\partial f_{\hat{a}}^{(3)}}{\partial\sigma_j} = \frac{\partial \mathbf{C}_{\hat{a}}}{\partial\sigma_j}\cdot\bar{\ell}_{\rm obs}^{(3)} + (\mathbf{v}\cdot\bar{\ell}_{\varnothing})\frac{\partial f_{\hat{a}}^{(2)}}{\partial\sigma_j} + 2h_{\rm obs}\frac{\partial f_{\hat{a}}^{(1)}}{\partial\sigma_j} + [h_{\rm obs}(\mathbf{v}\cdot\bar{\ell}_{\varnothing}) + \mathbf{v}\cdot\bar{\ell}_{\rm obs}^{(2)}]\frac{\partial f_{\hat{a}}^{(0)}}{\partial\sigma_j},
\end{aligned} \tag{C1}$$

with

$$\begin{aligned}
&\frac{\partial C_{\hat{1}}^1}{\partial\sigma_1} = \frac{32\sigma_1(\sigma_2^2+\sigma_3^2)}{(2-\Sigma)^3} \qquad \frac{\partial C_{\hat{1}}^1}{\partial\sigma_2} = -\frac{16\sigma_2(\sigma_1^2-\sigma_2^2-\sigma_3^2+1)}{(2-\Sigma)^3}, \qquad \frac{\partial C_{\hat{1}}^1}{\partial\sigma_3} = -\frac{16\sigma_3(\sigma_1^2-\sigma_2^2-\sigma_3^2+1)}{(2-\Sigma)^3},\\
&\frac{\partial C_{\hat{1}}^2}{\partial\sigma_1} = -\frac{8[(-3\sigma_2+\sigma_1\sigma_3)\Sigma + 2\sigma_2 - 4\sigma_2^3 - 4\sigma_2\sigma_3^2 + 2\sigma_1\sigma_3]}{(2-\Sigma)^3}, \qquad \frac{\partial C_{\hat{1}}^2}{\partial\sigma_2} = -\frac{8[(\sigma_2\sigma_3+\sigma_1)\Sigma + 4\sigma_1\sigma_2^2 + 2\sigma_2\sigma_3 - 2\sigma_1]}{(2-\Sigma)^3},\\
&\frac{\partial C_{\hat{1}}^2}{\partial\sigma_3} = -\frac{4[\Sigma^2 + (-2+2\sigma_3^2)\Sigma + 8\sigma_2\sigma_3\sigma_1 + 4\sigma_3^2]}{(2-\Sigma)^3}, \qquad \frac{\partial C_{\hat{1}}^3}{\partial\sigma_1} = \frac{8[(3\sigma_3+\sigma_1\sigma_2)\Sigma - 2\sigma_3 + 4\sigma_3\sigma_2^2 + 4\sigma_3^3 + 2\sigma_1\sigma_2]}{(2-\Sigma)^3},\\
&\frac{\partial C_{\hat{1}}^3}{\partial\sigma_2} = \frac{4[\Sigma^2 + (-2+2\sigma_2^2)\Sigma - 8\sigma_2\sigma_3\sigma_1 + 4\sigma_2^2]}{(2-\Sigma)^3}, \qquad \frac{\partial C_{\hat{1}}^3}{\partial\sigma_3} = -\frac{8[(\sigma_1-\sigma_2\sigma_3)\Sigma + 4\sigma_1\sigma_3^2 - 2\sigma_2\sigma_3 - 2\sigma_1]}{(2-\Sigma)^3},
\end{aligned} \tag{C2}$$

and

$$\begin{aligned}
&\frac{\partial C_{\hat{3}}^1}{\partial\sigma_1} = -\frac{8[(-3\sigma_3+\sigma_1\sigma_2)\Sigma + 2\sigma_3 - 4\sigma_3\sigma_2^2 - 4\sigma_3^3 + 2\sigma_1\sigma_2]}{(2-\Sigma)^3}, \qquad \frac{\partial C_{\hat{3}}^1}{\partial\sigma_2} = -\frac{4[\Sigma^2 + (-2+2\sigma_2^2)\Sigma + 8\sigma_2\sigma_3\sigma_1 + 4\sigma_2^2]}{(2-\Sigma)^3},\\
&\frac{\partial C_{\hat{3}}^1}{\partial\sigma_3} = -\frac{8[(\sigma_2\sigma_3+\sigma_1)\Sigma + 4\sigma_1\sigma_3^2 + 2\sigma_2\sigma_3 - 2\sigma_1]}{(2-\Sigma)^3}, \qquad \frac{\partial C_{\hat{3}}^2}{\partial\sigma_1} = -\frac{4[\Sigma^2 + (4+2\sigma_2^2+2\sigma_3^2)\Sigma + 8\sigma_2\sigma_3\sigma_1 - 4 + 4\sigma_2^2 + 4\sigma_3^2]}{(2-\Sigma)^3},\\
&\frac{\partial C_{\hat{3}}^2}{\partial\sigma_2} = \frac{8[(-\sigma_3+\sigma_1\sigma_2)\Sigma - 4\sigma_3\sigma_2^2 + 2\sigma_1\sigma_2 + 2\sigma_3]}{(2-\Sigma)^3}, \qquad \frac{\partial C_{\hat{3}}^2}{\partial\sigma_3} = \frac{8[(-\sigma_2+\sigma_1\sigma_3)\Sigma - 4\sigma_2\sigma_3^2 + 2\sigma_1\sigma_3 + 2\sigma_2]}{(2-\Sigma)^3},\\
&\frac{\partial C_{\hat{3}}^3}{\partial\sigma_1} = \frac{16\sigma_1(\sigma_1^2+\sigma_2^2-\sigma_3^2-1)}{(2-\Sigma)^3}, \qquad \frac{\partial C_{\hat{3}}^3}{\partial\sigma_2} = \frac{16\sigma_2(\sigma_1^2+\sigma_2^2-\sigma_3^2-1)}{(2-\Sigma)^3}, \qquad \frac{\partial C_{\hat{3}}^3}{\partial\sigma_3} = \frac{32\sigma_3(\sigma_1^2+\sigma_2^2)}{(2-\Sigma)^3},
\end{aligned} \tag{C3}$$

as from Eq. (56).

APPENDIX D: APPROXIMATED RELATIONSHIPS FOR THE EXPRESSIONS OF THE DERIVATIVES

$$\frac{f_{\hat{1}}^{(0)}}{\cos\phi^{(0)}}\frac{\partial\cos\phi^{(0)}}{\partial p_j}=\frac{\partial f_{\hat{1}}^{(0)}}{\partial p_j}+\cos^2\phi^{(0)}\frac{f_{\hat{3}}^{(0)}}{f_{\hat{1}}^{(0)}}\frac{\partial f_{\hat{3}}^{(0)}}{\partial p_j},$$

$$\frac{f_{\hat{1}}^{(0)}}{\cos\phi^{(0)}}\frac{\partial\cos\phi^{(1)}}{\partial p_j}=\frac{\partial f_{\hat{1}}^{(1)}}{\partial p_j}+\cos^2\phi^{(0)}\frac{f_{\hat{3}}^{(0)}}{f_{\hat{1}}^{(0)}}\frac{\partial f_{\hat{3}}^{(1)}}{\partial p_j}+\cos^2\phi^{(0)}\frac{f_{\hat{3}}^{(0)}f_{\hat{3}}^{(1)}}{(f_{\hat{1}}^{(0)})^2}\frac{\partial f_{\hat{1}}^{(0)}}{\partial p_j}+\left[\cos^2\phi^{(0)}\frac{f_{\hat{3}}^{(1)}}{f_{\hat{1}}^{(0)}}+\frac{f_{\hat{3}}^{(0)}f_{\hat{1}}^{(1)}}{(f_{\hat{1}}^{(0)})^2}+3\cos^4\phi^{(0)}\frac{(f_{\hat{3}}^{(0)})^2f_{\hat{3}}^{(1)}}{(f_{\hat{1}}^{(0)})^3}\right]\frac{\partial f_{\hat{3}}^{(0)}}{\partial p_j},$$

$$\begin{aligned}\frac{f_{\hat{1}}^{(0)}}{\cos\phi^{(0)}}\frac{\partial\cos\phi^{(2)}}{\partial p_j}=&\frac{\partial f_{\hat{1}}^{(2)}}{\partial p_j}+\cos^2\phi^{(0)}\frac{f_{\hat{3}}^{(0)}}{f_{\hat{1}}^{(0)}}\frac{\partial f_{\hat{3}}^{(2)}}{\partial p_j}+\cos^2\phi^{(0)}\frac{f_{\hat{3}}^{(0)}f_{\hat{3}}^{(1)}}{(f_{\hat{1}}^{(0)})^2}\frac{\partial f_{\hat{1}}^{(1)}}{\partial p_j}\\&+\left[\cos^2\phi^{(0)}\frac{f_{\hat{3}}^{(0)}f_{\hat{1}}^{(1)}}{(f_{\hat{1}}^{(0)})^2}+\cos^4\phi^{(0)}\frac{f_{\hat{3}}^{(1)}}{(f_{\hat{1}}^{(0)})^3}(1+2(f_{\hat{3}}^{(0)})^2)\right]\frac{\partial f_{\hat{3}}^{(1)}}{\partial p_j}\\&+\left[\cos^2\phi^{(0)}\frac{f_{\hat{3}}^{(0)}f_{\hat{3}}^{(2)}}{(f_{\hat{1}}^{(0)})^2}+\cos^4\phi^{(0)}\frac{(f_{\hat{3}}^{(1)})^2}{(f_{\hat{1}}^{(0)})^4}\left(1+\frac{1}{2}(f_{\hat{3}}^{(0)})^2\right)\right]\frac{\partial f_{\hat{1}}^{(0)}}{\partial p_j}+\left[\cos^2\phi^{(0)}\left(\frac{f_{\hat{3}}^{(2)}}{f_{\hat{1}}^{(0)}}+\frac{f_{\hat{3}}^{(1)}f_{\hat{1}}^{(1)}}{(f_{\hat{1}}^{(0)})^2}+\frac{f_{\hat{3}}^{(0)}f_{\hat{1}}^{(2)}}{(f_{\hat{1}}^{(0)})^2}\right)\right.\\&\left.+3\cos^4\phi^{(0)}\frac{(f_{\hat{3}}^{(0)})^2}{(f_{\hat{1}}^{(0)})^4}\left(f_{\hat{1}}^{(1)}f_{\hat{3}}^{(1)}+f_{\hat{1}}^{(0)}f_{\hat{3}}^{(2)}+\frac{2f_{\hat{1}}^{(0)}}{3f_{\hat{3}}^{(0)}}(f_{\hat{3}}^{(1)})^2\right)+\frac{5}{2}\cos^6\phi^{(0)}\frac{f_{\hat{3}}^{(0)}(f_{\hat{3}}^{(1)})^2}{(f_{\hat{1}}^{(0)})^5}(1+2(f_{\hat{3}}^{(0)})^2)\right]\frac{\partial f_{\hat{3}}^{(0)}}{\partial p_j},\end{aligned}$$

$$\begin{aligned}\frac{f_{\hat{1}}^{(0)}}{\cos\phi^{(0)}}\frac{\partial\cos\phi^{(3)}}{\partial p_j}=&\frac{\partial f_{\hat{1}}^{(3)}}{\partial p_j}+\cos^2\phi^{(0)}\frac{f_{\hat{3}}^{(0)}}{f_{\hat{1}}^{(0)}}\frac{\partial f_{\hat{3}}^{(3)}}{\partial p_j}+\cos^2\phi^{(0)}\frac{f_{\hat{3}}^{(0)}f_{\hat{3}}^{(1)}}{(f_{\hat{1}}^{(0)})^2}\frac{\partial f_{\hat{1}}^{(2)}}{\partial p_j}\\&+\left[\cos^2\phi^{(0)}\frac{f_{\hat{3}}^{(0)}f_{\hat{1}}^{(1)}}{(f_{\hat{1}}^{(0)})^2}+\cos^4\phi^{(0)}\frac{f_{\hat{3}}^{(1)}}{(f_{\hat{1}}^{(0)})^3}(1+2(f_{\hat{3}}^{(0)})^2)\right]\frac{\partial f_{\hat{3}}^{(2)}}{\partial p_j}\\&+\left[\cos^2\phi^{(0)}\frac{f_{\hat{3}}^{(0)}f_{\hat{3}}^{(2)}}{(f_{\hat{1}}^{(0)})^2}+\cos^4\phi^{(0)}\frac{(f_{\hat{3}}^{(1)})^2}{(f_{\hat{1}}^{(0)})^4}\left(1+\frac{1}{2}(f_{\hat{3}}^{(0)})^2\right)\right]\frac{\partial f_{\hat{1}}^{(1)}}{\partial p_j}\\&+\left[\cos^2\phi^{(0)}\frac{f_{\hat{3}}^{(0)}f_{\hat{1}}^{(2)}}{(f_{\hat{1}}^{(0)})^2}+\cos^4\phi^{(0)}\frac{1}{(f_{\hat{1}}^{(0)})^4}(1+2(f_{\hat{3}}^{(0)})^2)(f_{\hat{3}}^{(2)}f_{\hat{1}}^{(0)}+f_{\hat{1}}^{(1)}f_{\hat{3}}^{(1)})\right.\\&\left.+\frac{3}{2}\cos^6\phi^{(0)}\frac{f_{\hat{3}}^{(0)}(f_{\hat{3}}^{(1)})^2}{(f_{\hat{1}}^{(0)})^5}(3+2(f_{\hat{3}}^{(0)})^2)\right]\frac{\partial f_{\hat{3}}^{(1)}}{\partial p_j}+\left[\cos^2\phi^{(0)}\frac{f_{\hat{3}}^{(0)}f_{\hat{3}}^{(3)}}{(f_{\hat{1}}^{(0)})^2}+\cos^4\phi^{(0)}\frac{f_{\hat{3}}^{(1)}f_{\hat{3}}^{(2)}}{(f_{\hat{1}}^{(0)})^4}(1+2(f_{\hat{3}}^{(0)})^2)\right.\\&\left.+\frac{1}{2}\cos^6\phi^{(0)}\frac{f_{\hat{3}}^{(0)}(f_{\hat{3}}^{(1)})^3}{(f_{\hat{1}}^{(0)})^6}(3+2(f_{\hat{3}}^{(0)})^2)\right]\frac{\partial f_{\hat{1}}^{(0)}}{\partial p_j}+\left\{\cos^2\phi^{(0)}\frac{1}{(f_{\hat{1}}^{(0)})^2}(f_{\hat{1}}^{(0)}f_{\hat{3}}^{(3)}+f_{\hat{1}}^{(1)}f_{\hat{3}}^{(2)}+f_{\hat{1}}^{(2)}f_{\hat{3}}^{(1)}+f_{\hat{1}}^{(3)}f_{\hat{3}}^{(0)})\right.\\&+3\cos^4\phi^{(0)}\frac{(f_{\hat{3}}^{(0)})^2}{(f_{\hat{1}}^{(0)})^4}\left[f_{\hat{1}}^{(0)}f_{\hat{3}}^{(3)}+f_{\hat{1}}^{(1)}f_{\hat{3}}^{(2)}+f_{\hat{1}}^{(2)}f_{\hat{3}}^{(1)}+\frac{2f_{\hat{3}}^{(1)}}{3f_{\hat{3}}^{(0)}}(f_{\hat{1}}^{(1)}f_{\hat{3}}^{(1)}+2f_{\hat{1}}^{(0)}f_{\hat{3}}^{(2)})\right]\\&+\frac{1}{2}\cos^6\phi^{(0)}\frac{f_{\hat{3}}^{(1)}}{(f_{\hat{1}}^{(0)})^6}(1+2(f_{\hat{3}}^{(0)})^2)[5f_{\hat{3}}^{(0)}(f_{\hat{1}}^{(1)}f_{\hat{3}}^{(1)}+2f_{\hat{1}}^{(0)}f_{\hat{3}}^{(2)})+3f_{\hat{1}}^{(0)}(f_{\hat{3}}^{(1)})^2]\\&\left.+\frac{7}{2}\cos^8\phi^{(0)}\frac{(f_{\hat{3}}^{(0)})^2(f_{\hat{3}}^{(1)})^3}{(f_{\hat{1}}^{(0)})^7}(3+2(f_{\hat{3}}^{(0)})^2)\right\}\frac{\partial f_{\hat{3}}^{(0)}}{\partial p_j}.\end{aligned}\tag{D1}$$

[1] T. Prusti, J. H. J. de Bruijne, A. G. A. Brown *et al.* (Gaia Collaboration). Astron. Astrophys. **36**, A1 (2016).
[2] A. C. Perryman, K. S. de Boer, G. Gilmore, E. Høg, M. G. Lattanzi, L. Lindegren, X. Luri, F. Mignard, O. Pace, and P. T. de Zeeuw, Astron. Astrophys. **369**, 339 (2001).
[3] M. G. Lattanzi, Mem. Soc. Astron. Ital. **83**, 1033 (2012).
[4] A. G. A. Brown, *et al.* Gaia Collaboration). Astron. Astrophys. **595**, A2 (2016).
[5] L. Lindegren, U. Lammers, U. Bastian *et al.* (Gaia Collaboration), Astron. Astrophys. **595**, A4 (2016).
[6] F. de Felice and D. Bini, *Classical Measurements in Curved Space-Times* Series: Cambridge Monographs on Mathematical Physics (Cambridge University Press, Cambridge, England, 2010).
[7] DPAC: Proposal for the Gaia Data Processing, edited by F. Mignard and R. Drimmel, Gaia Tech. Rep. No. GAIA-CD-SP-DPAC-FM-030-2, ESA, http://www.rssd.esa.int/cs/livelink/open/2720336
[8] D. Michalik, L. Lindegren, and D. Hobbs, Astron. Astrophys. **574**, A115 (2015).
[9] M. Bandieramonte, U. Becciani, A. Vecchiato, M. G. Lattanzi, and B. Bucciarelli, *2012 IEEE 21st International Workshop on Enabling Technologies: Infrastructure for Collaborative Enterprises* (IEEE Computer Society, Washington, DC, 2012), pp 167–172
[10] A. Vecchiato *et al.* Astron. Astrophys. (to be published).
[11] A. Vecchiato, U. Abbas, B. Bucciarelli, M. G. Lattanzi, and R. Morbidelli, in *Proceedings of the International Astronomical Union, Symposium S261.*
[12] A. Vecchiato, M. G. Lattanzi, B. Bucciarelli, M. Crosta, F. de Felice, and M. Gai, Astron. Astrophys. **399**, 337 (2003).
[13] M. Crosta, A. Vecchiato, F. de Felice, and M. G. Lattanzi, Classical Quantum Gravity **32**, 165008 (2015).
[14] M. Soffel *et al.*, Astrophys. J. **126**, 2687 (2003).
[15] P. Teyssandier and C. Le Poncin-Lafitte, Classical Quantum Gravity **25**, 145020 (2008).
[16] S. Zschocke, Phys. Rev. D **94**, 122001 (2016).
[17] S. M. Kopeikin and G. Schaefer, Phys. Rev. D **60**, 124002 (1999).
[18] T. Damour, M. Soffel, and C. Xu, Phys. Rev. D **43**, 3273 (1991).
[19] S. Klioner, Astron. Astrophys. **404**, 783 (2003).
[20] A. Hees, S. Bertone, and C. Le Poncin-Lafitte, Phys. Rev. D **89**, 064045 (2014).
[21] S. Zschocke and M. H. Soffel, Classical Quantum Gravity **31**, 175001 (2014).
[22] F. de Felice, M. Crosta, A. Vecchiato, M. G. Lattanzi, and B. Bucciarelli, Astron. J. **607**, 580 (2004).
[23] M. Crosta, Classical Quantum Gravity **28**, 235013 (2011).
[24] F. de Felice, A. Vecchiato, M. Crosta, B. Bucciarelli, and M. G. Lattanzi, Astron. J. **653**, 1552 (2006).
[25] S. Bertone, O. Minazzoli, M. Crosta, C. Le Poncin-Lafitte, A. Vecchiato, and M.-C. Angonin, Classical Quantum Gravity **31**, 015021 (2014).
[26] M. Crosta and A. Vecchiato, Astron. Astrophys. **509**, A37 (2010).
[27] D. Bini, M. Crosta, and F. de Felice, Classical Quantum Gravity **20**, 4695 (2003).
[28] L. Bianchi, A. Vecchiato, and B. Bucciarelli, http://www.rssd.esa.int/llink/livelink/open/305921.
[29] T. Damour and B. R. Iyer, Phys. Rev. D **43**, 3259 (1991).